



The Thermodynamics of Naturally Heated Coronal Null Points

Daniel Johnson,

Alan Hood, Peter Cargill,

Craig Johnston, Jack Reid, Gert Botha, Ben Snow



Outline

- Accuracy of numerical treatments
- Thermal conduction about nulls
- Heating null points
- Equilibrium Thermal Structure
- Numerical, physical or both?

- Cooling X-Points

- 'Real' heating and cooling
- Photospheric Driving



The thermodynamic response of heating at coronal null points

D. Johnson¹*, A. W. Hood¹, P. J. Cargill^{1,2}, J. Reid¹ and C. D. Johnston^{3,4}

¹*School of Mathematics and Statistics, University of St Andrews, St Andrews, Fife KY16 9SS, UK*

²*The Blackett Laboratory, Imperial College, London SW7 2BW, UK*

³*Department of Physics and Astronomy, George Mason University, Fairfax, VA 22030, USA*

⁴*NASA Goddard Space Flight Center, Greenbelt, MD 20771, USA*

Accepted 2024 July 15. Received 2024 July 11; in original form 2024 May 3

ABSTRACT

Magnetic null points are an important aspect of the magnetic field structure of the solar corona and can be sites of enhanced dissipation. This paper uses analytical and numerical models to investigate the plasma structure around a heated null. It is shown that the temperature profile not only differs significantly from that in a uniform field, but also that the profile depends significantly on the spatial structure of the heating. Field lines close to the separatrices and the null point have higher temperatures than a uniform field for the same heating input. The dependence of the results near the null on both the ratio of perpendicular to parallel conduction, and numerical resolution is also explored. The comparison between analytic and numerical solutions also provides a useful benchmark to compare MHD codes with anisotropic thermal conduction.

Key words: conduction – Sun: corona – Sun: magnetic fields.

1 INTRODUCTION

The heating of the solar corona is a highly topical research area and several possible heating mechanisms have been suggested (e.g. Heyvaerts & Priest 1983; Klimchuk 2006; Van Doorselaere, Andries & Poedts 2007; Hood, Browning & Van der Linden 2009; Parnell & De Moortel 2012; De Moortel & Browning 2015). One is the dissipation of hydromagnetic waves which we discuss in Section 5. An alternative (e.g. Parker 1972; Cargill, Warren & Bradshaw 2015) is that magnetic energy is slowly stored in the coronal magnetic field and released in a series of small reconnection events, often termed ‘nanoflares’ (e.g. Parker 1988). This is commonly discussed in terms of field line braiding (e.g. Zaker & Cleveland 1993; Pontin et al. 2016), where the local magnetic field becomes mis-aligned, permitting reconnection, which in turn leads to heating and particle acceleration in the vicinity of the reconnection site. In terms of the plasma properties, for quasi-steady heating, an equilibrium is attained among the heating, thermal conduction and optically thin radiation (e.g. Rosner, Tucker & Vaiana 1978), though footpoint heating can lead to different outcomes (e.g. Antiochos & Klimchuk 1991; Froment et al. 2018). For impulsive heating, defined as arising when the duration of the heating is shorter than the characteristic timescale of plasma cooling, the plasma first cools by conduction, then by radiation (e.g. Cargill, Mariska & Antiochos 1995). The conductive cooling time scales as $T^{-3/2}$ and, for typical active region parameters, it is of order a few hundred seconds, shorter than cooling due to optically thin radiation at such temperatures. However, if very high temperatures, of order 10 MK, are reached, as suggested by some observations (e.g. Reale et al. 2009; Testa & Reale 2012;

Parenti et al. 2017), the cooling of hot plasma is very rapid in such braided fields, and this poses major challenges for detectability (e.g. Barnes, Cargill & Bradshaw 2016).

There is though another coronal magnetic configuration associated with dissipation, namely a magnetic null point (e.g. Lau & Finn 1990; Parnell et al. 1996; Brown & Priest 2001). Their copious existence are inferred by Close, Parnell & Priest (2004), Régnier, Parnell & Haynes (2008), and Longcope & Parnell (2009) and observed by Cheng et al. (2023). Such null points are domains of weak magnetic field and it has been suggested (e.g. Galsgaard & Pontin 2011) that stressing the magnetic field near these points will result in the build-up of strong currents there, which then dissipate through direct plasma heating and (viscously damped) mass motions. Thus, heating associated with the null is not a local process, with a significant plasma volume being heated. While the build up and dissipation of magnetic energy at such nulls has been widely investigated (e.g. Craig & McClymont 1991; McLaughlin & Hood 2004, 2006; McLaughlin 2013), the thermodynamic response of the plasma to heating events, and to associated energy transport, in the neighbourhood of coronal null points has not been studied in any detail. That is the aim of this and subsequent papers.

In the strong field limit thermal conduction is aligned with the magnetic field (Braginskii 1965). However, the null introduces some potentially significant differences to conductive transport. Firstly, as the field around the null becomes small, thermal conduction must reduce to the isotropic form, while a full anisotropic conduction must be implemented elsewhere. Despite many magnetohydrodynamic (MHD) codes having implemented such an anisotropic heat conduction, there has been no quantification of how they cope with null points. Secondly, the magnetic field strength around the null is highly non-uniform. It is well known that the cross-section of a magnetic flux element has a significant influence on conductive

* E-mail: dj57@st-andrews.ac.uk

© 2024 The Author(s).

Published by Oxford University Press on behalf of Royal Astronomical Society. This is an Open Access article distributed under the terms of the Creative Commons Attribution License (<https://creativecommons.org/licenses/by/4.0/>), which permits unrestricted reuse, distribution, and reproduction in any medium, provided the original work is properly cited.



Outline

- Accuracy of numerical treatments
- Thermal conduction about nulls
- Heating null points
- Equilibrium Thermal Structure
- Numerical, physical or both?

- Cooling X-Points

- 'Real' heating and cooling
- Photospheric Driving



Working on corrections



Outline

- Accuracy of numerical treatments
- Thermal conduction about nulls
- Heating null points
- Equilibrium Thermal Structure
- Numerical, physical or both?

- Cooling X-Points

- 'Real' heating and cooling
- Photospheric Driving



Submitting very soon!



Paper 1

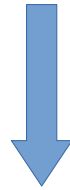


Thermal Conduction

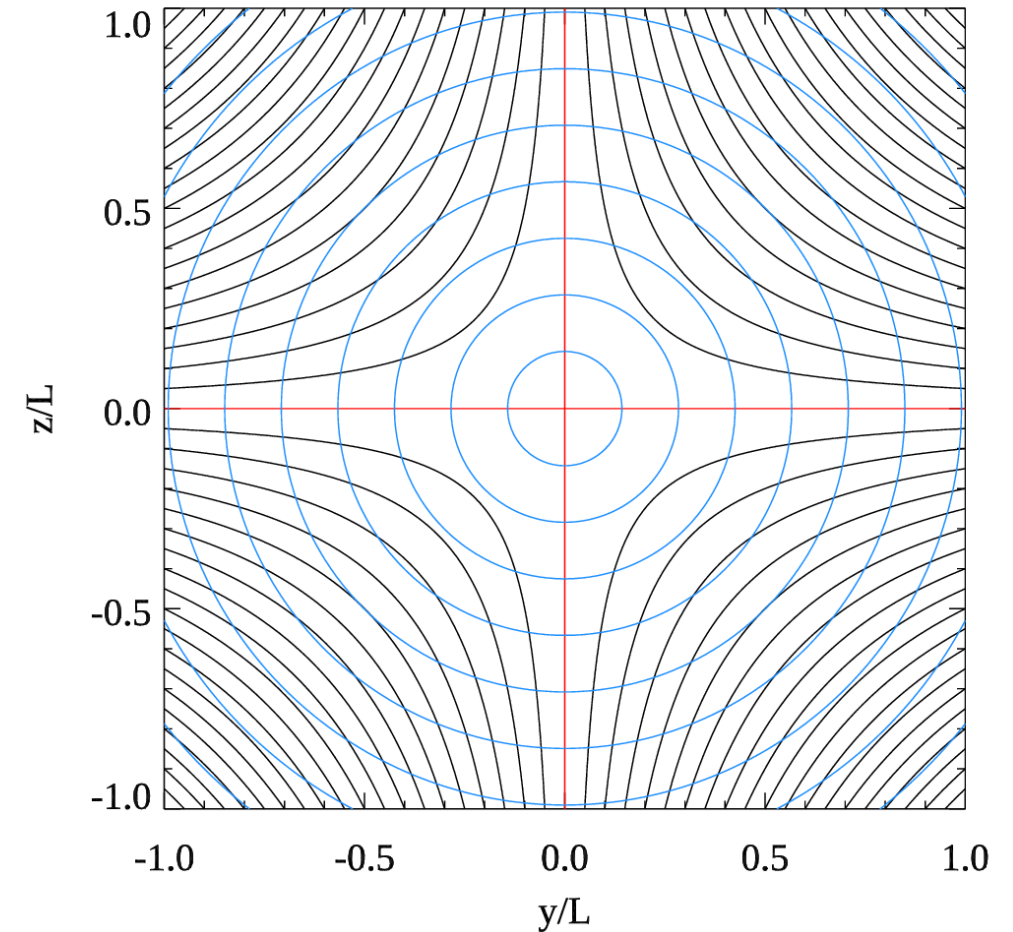


- Thermal conduction in a plasma with a strong magnetic field is highly anisotropic (Spitzer and Harm (1953), Braginskii (1965), Balescu (1988)).
- Fourier's law can be transformed with respect to the magnetic field.

$$\mathbf{q} = -\kappa \nabla T$$



$$\mathbf{q} = -\kappa_{\parallel} \nabla_{\parallel}(T) - \kappa_{\perp} \nabla_{\perp}(T)$$

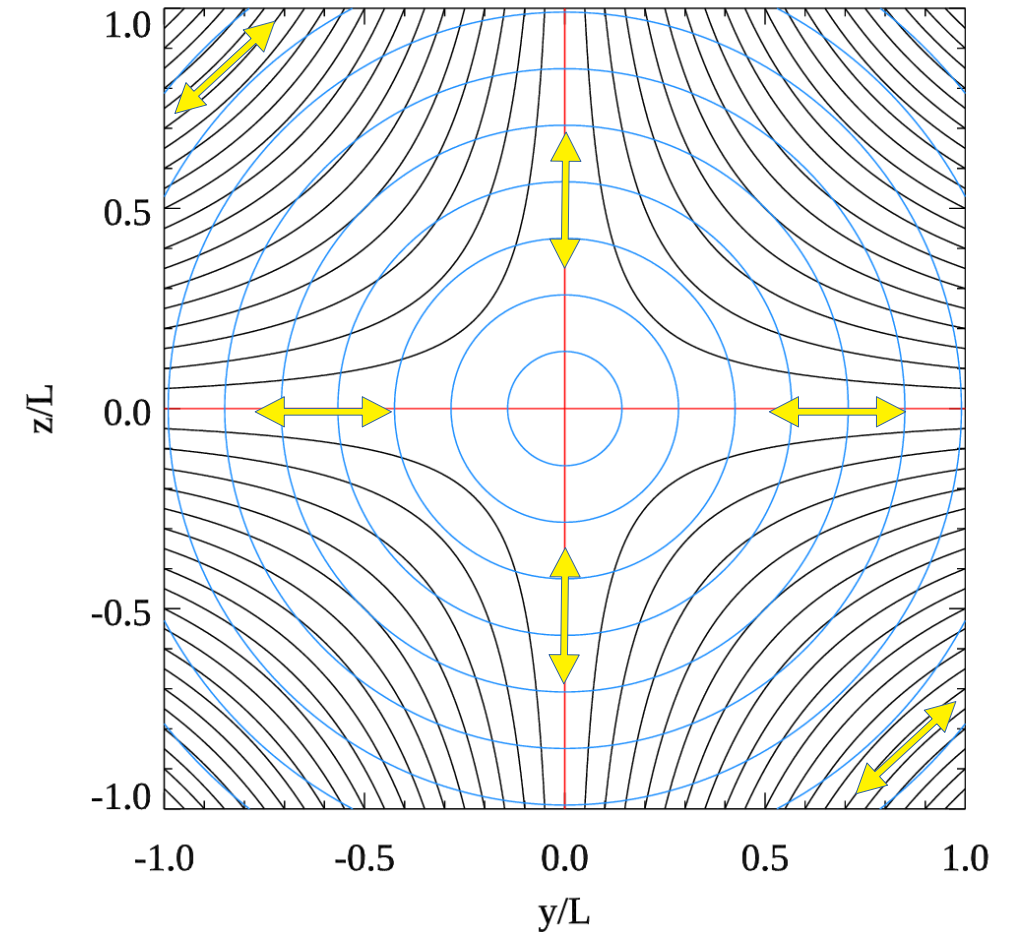




$$\kappa_{\parallel} = 3.2 \frac{nkT\tau}{m_e} \quad \kappa_{\perp} = 4.7 \frac{nkT}{m_e \Omega_e^2 \tau}$$

$$\Omega_e = 1.76 \times 10^7 \text{Bs}^{-1}$$

$$\frac{\kappa_{\parallel}}{\kappa_{\perp}} = \frac{3.2}{4.7} \tau^2 \Omega_e^2 \approx \tau^2 \Omega_e^2$$

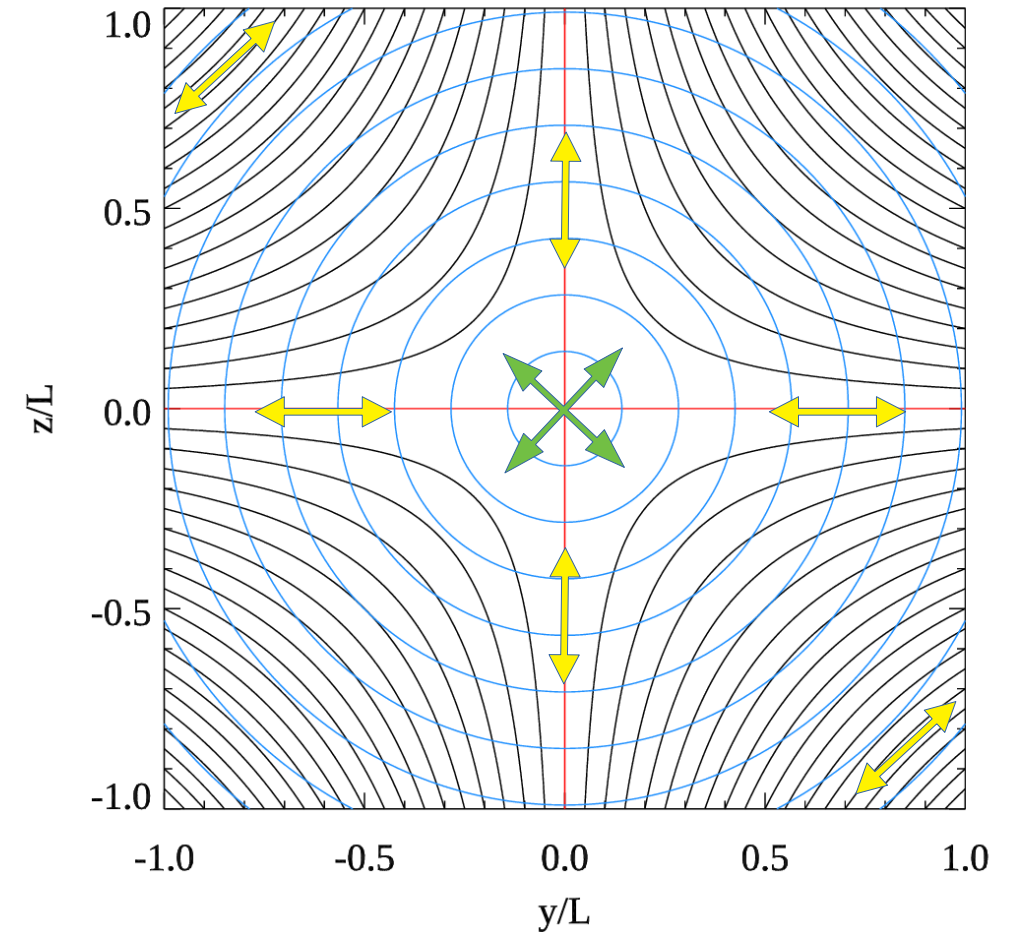




$$\kappa_{\parallel} = 3.2 \frac{nkT\tau}{m_e}$$

$$\kappa_{\perp} = 4.7 \frac{nkT}{m_e \Omega_e^2 \tau}$$

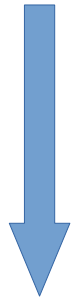
$$\frac{\kappa_{\parallel}}{\kappa_{\perp}} = 1$$



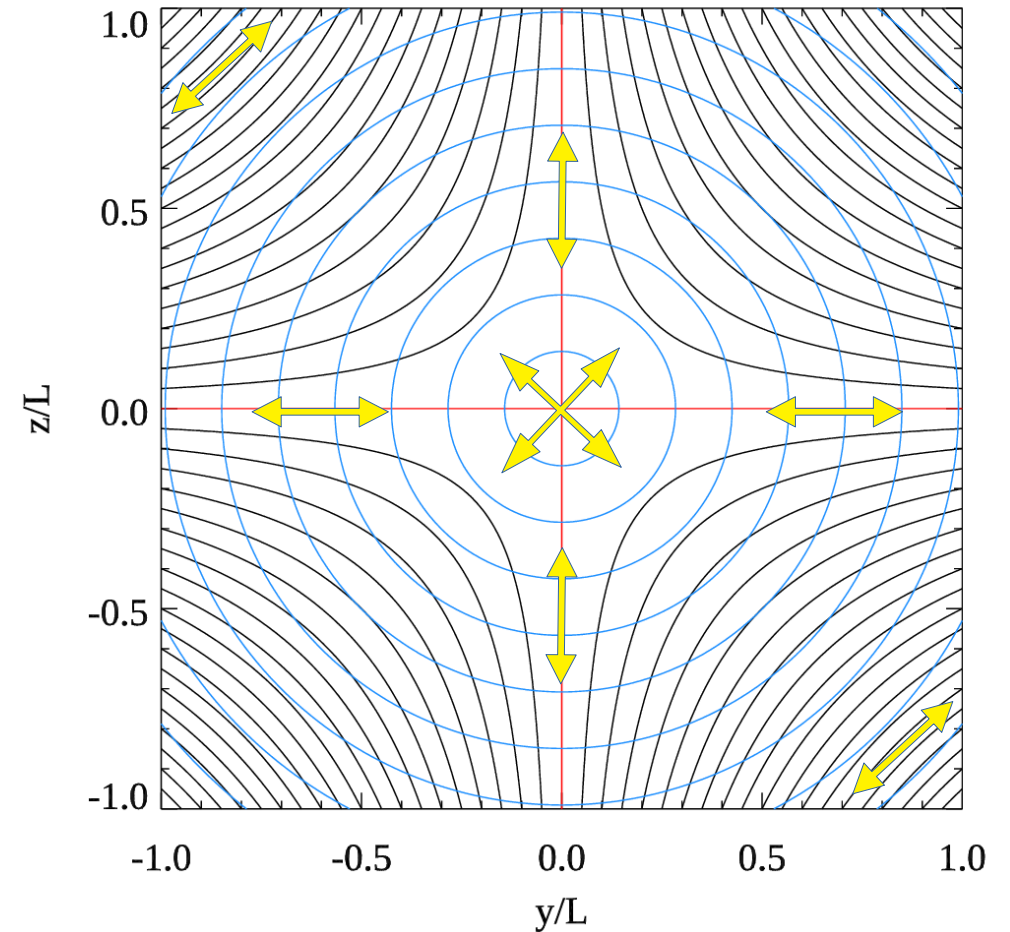


Lare3D – Numerical Treatment

$$\mathbf{q} = -\kappa_{\parallel} \nabla_{\parallel}(T) - \kappa_{\perp} \nabla_{\perp}(T)$$

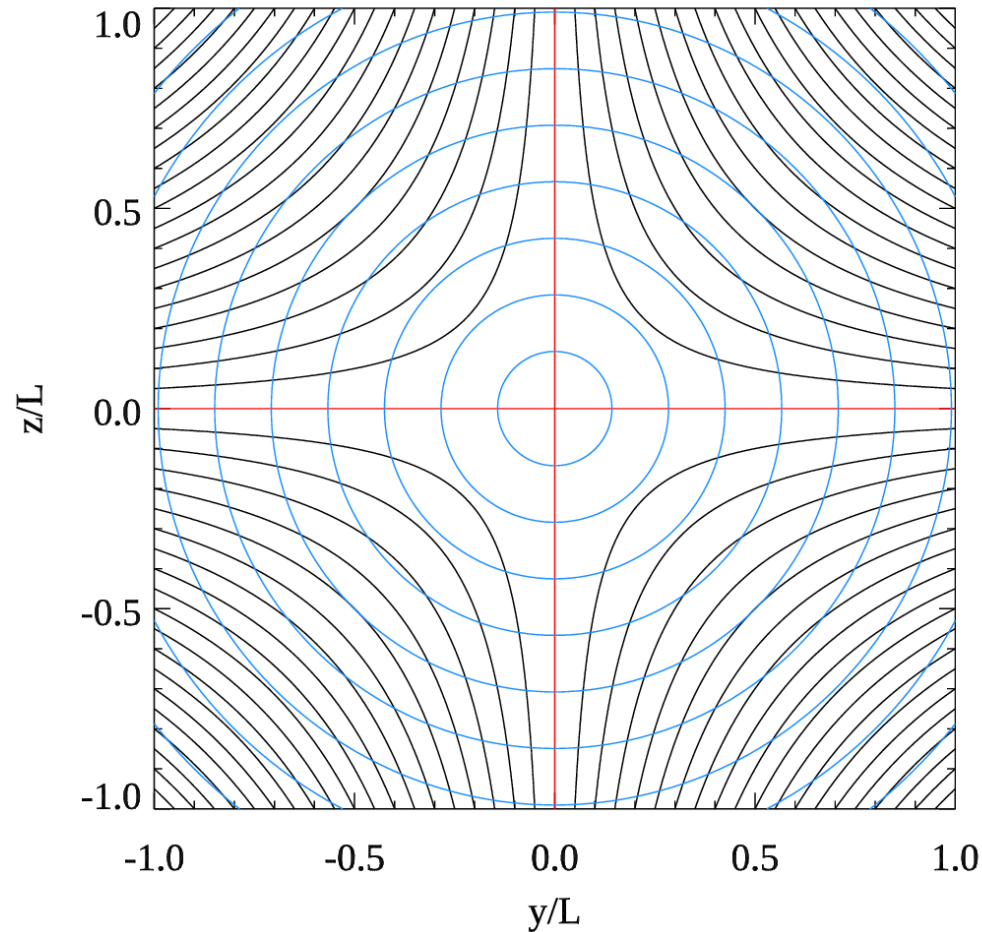


$$\mathbf{q} = \frac{\kappa_{\parallel}}{(B^2 + B_{min}^2)} (\mathbf{B} \cdot \nabla T) \mathbf{B} + \frac{B_{min}^2}{(B^2 + B_{min}^2)} \kappa_{\parallel} \nabla T$$





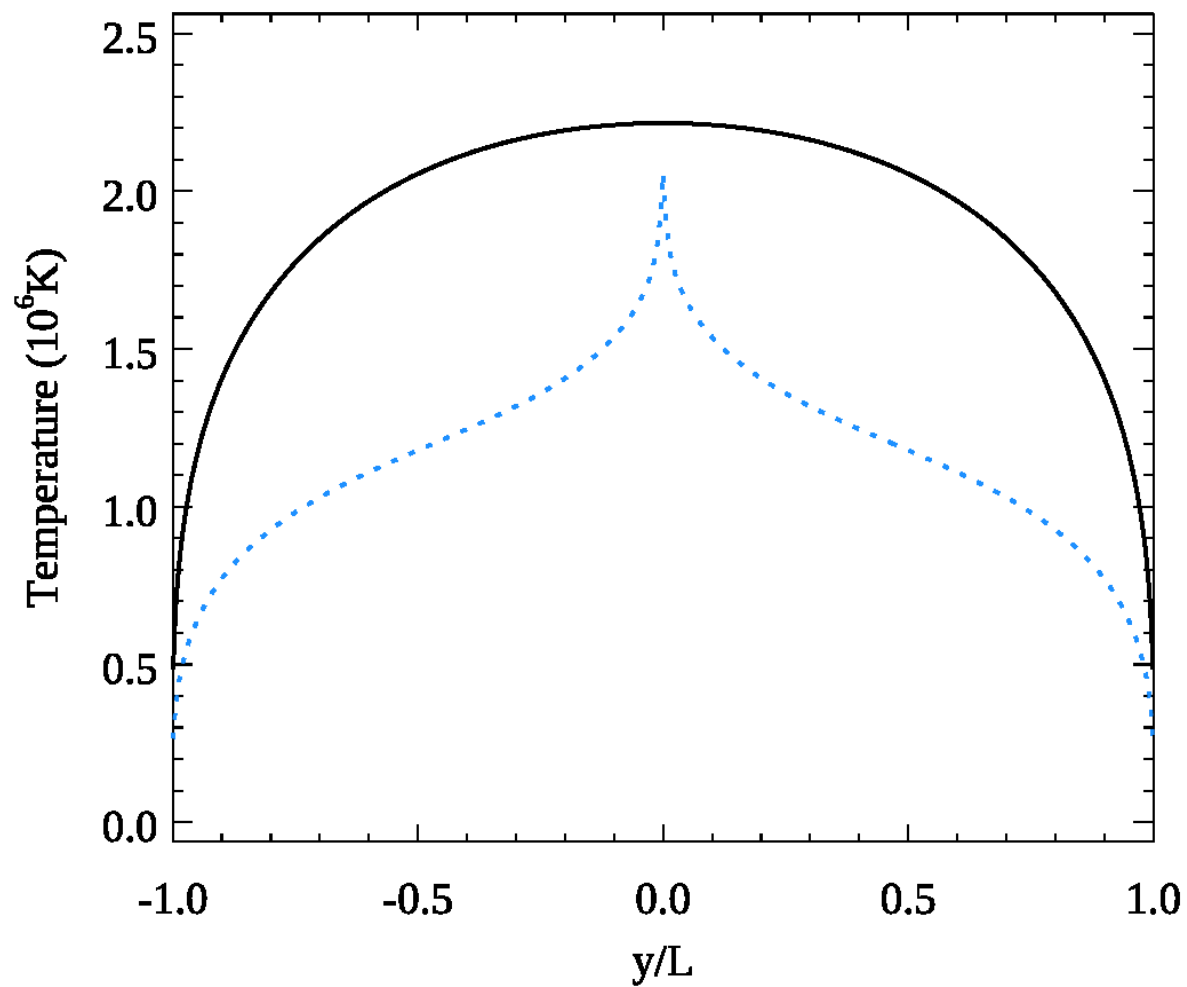
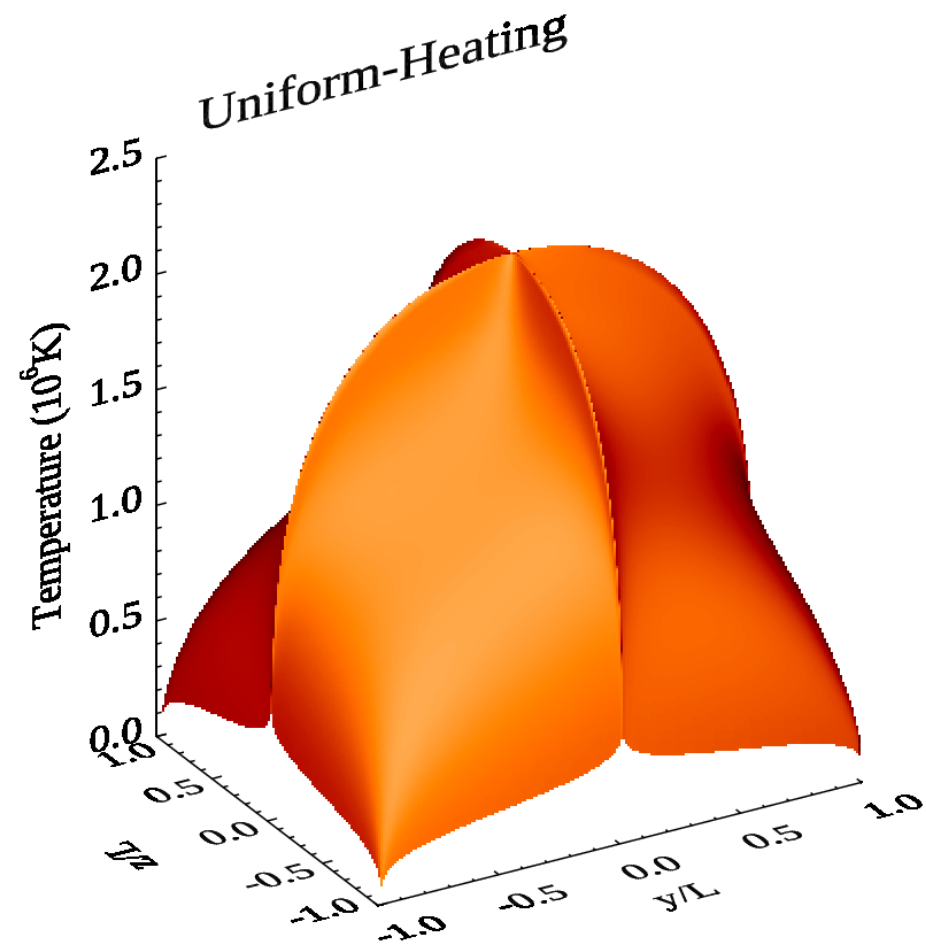
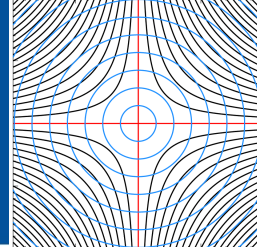
Thermodynamics of a Heated Null Point?

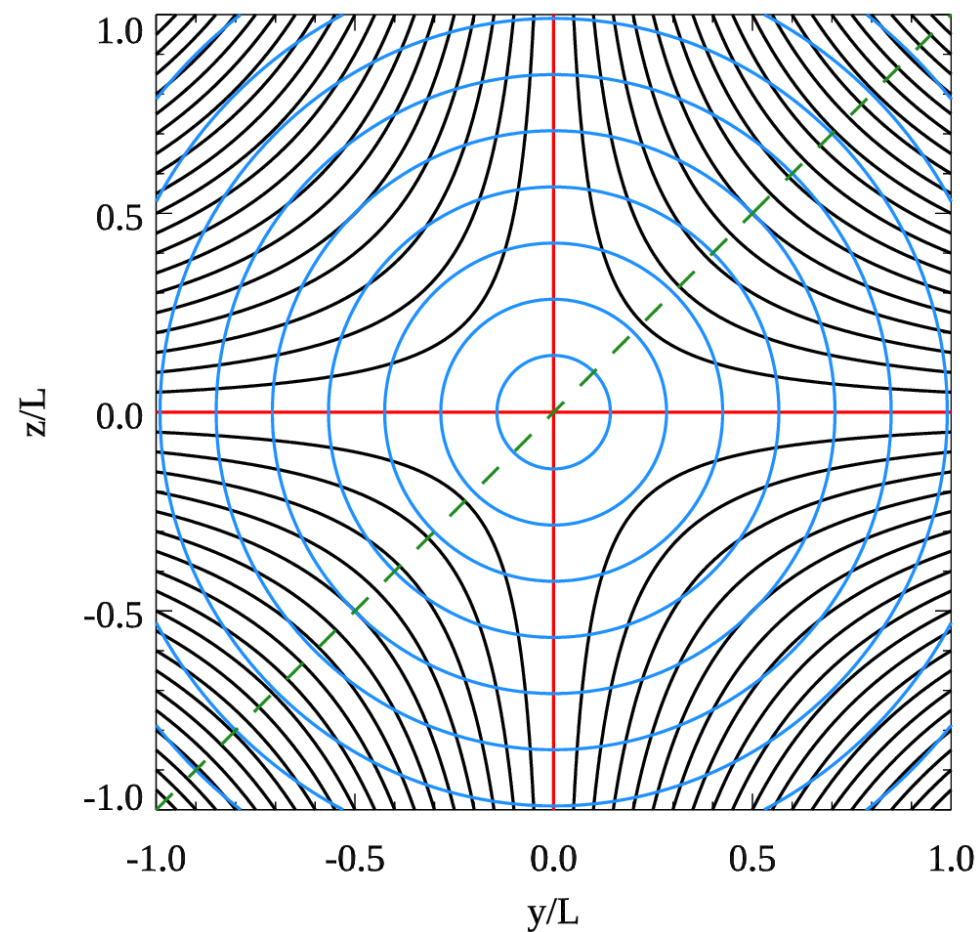
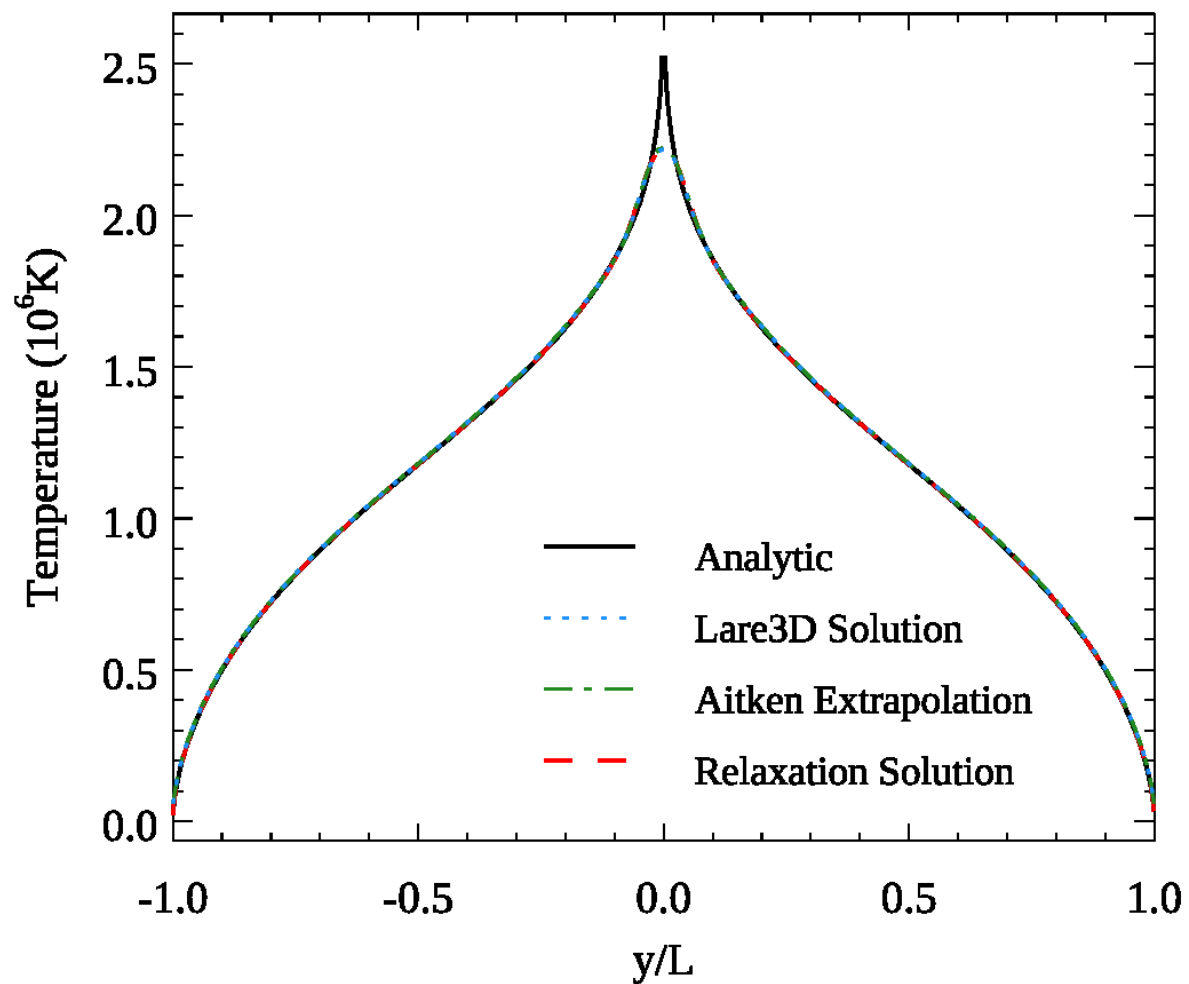


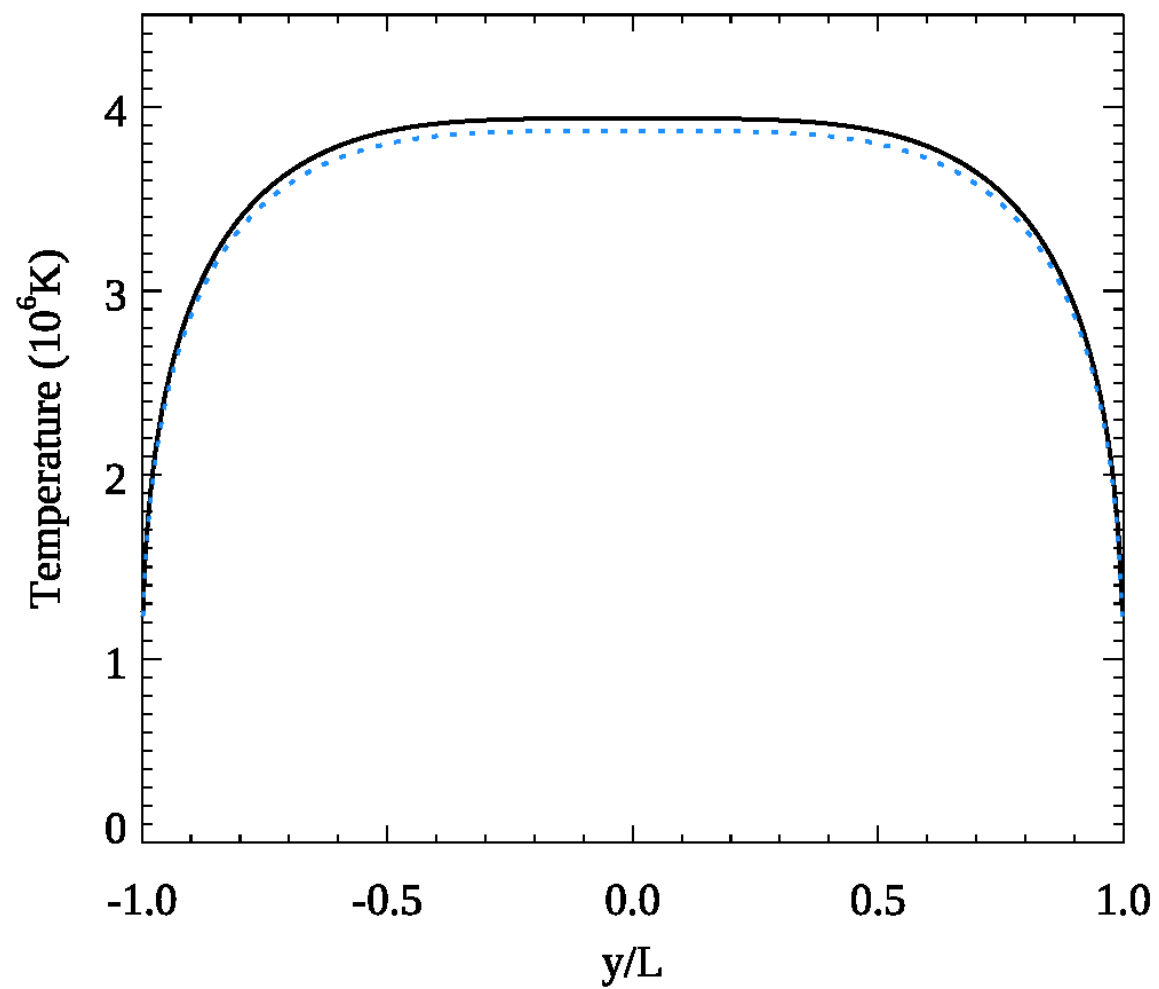
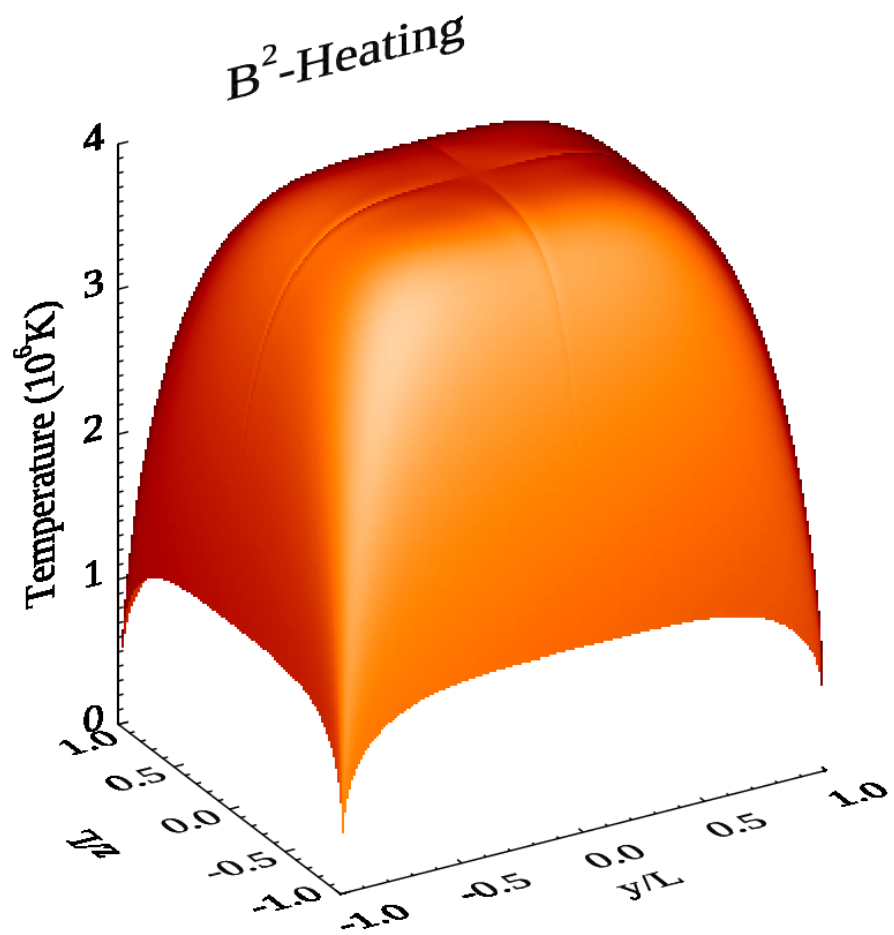
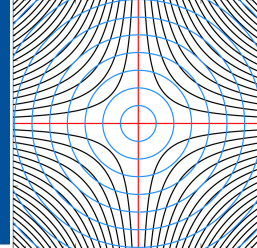
$$T = T_b \left(1 + \frac{7}{2} \frac{HL^2}{\kappa_0} F(y, z) \right)^{2/7}$$

$$G = G_0 - \frac{1}{4}(1 - y^2)(1 - z^2) \\ - \frac{1}{4}(1 + y^2)(1 - z^2) \ln |y| \\ - \frac{1}{4}(1 + z^2)(1 - y^2) \ln |z|$$

$$G = \frac{2}{7} \frac{\kappa_0}{L^2 H} T^{7/2}$$









Question: “Isn’t this all just numerical
and mathematical nonsense”

Tom Howson



Paper 2



Peter Cargill recognised that the solutions in Paper 1 can be used as solutions to estimate cooling, based on traditional techniques.

See Antiochos & Sturrock (1976) and Cargill et al. (2022) for details.



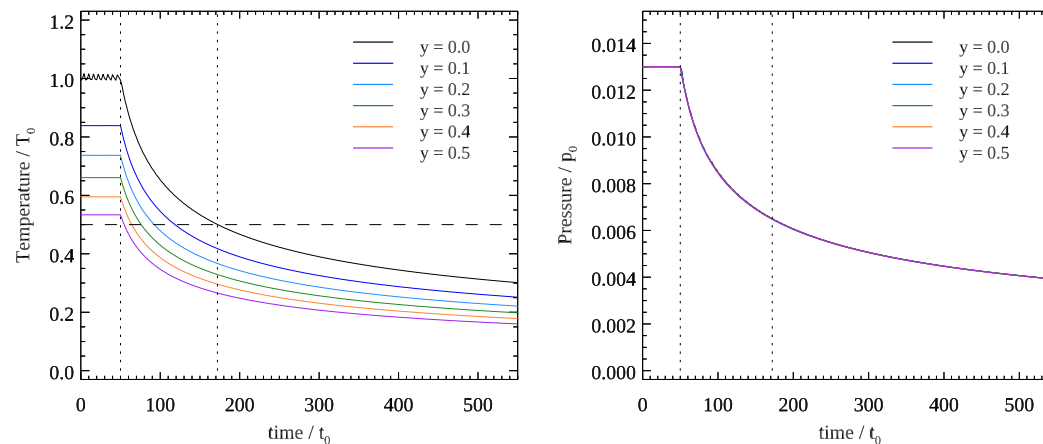
Nulls Cool Much More
Slowly than Straight Field



Nulls Tend to Cool in a Predictable Way



Uniform



B - Squared

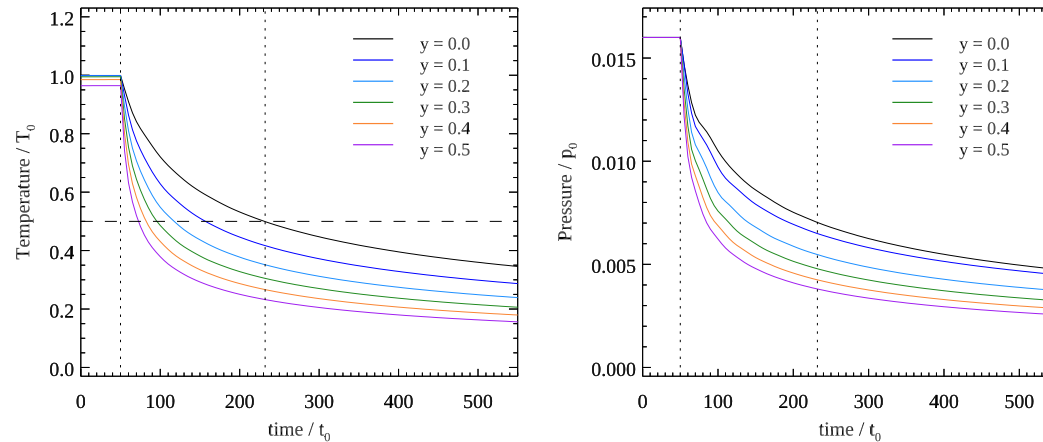
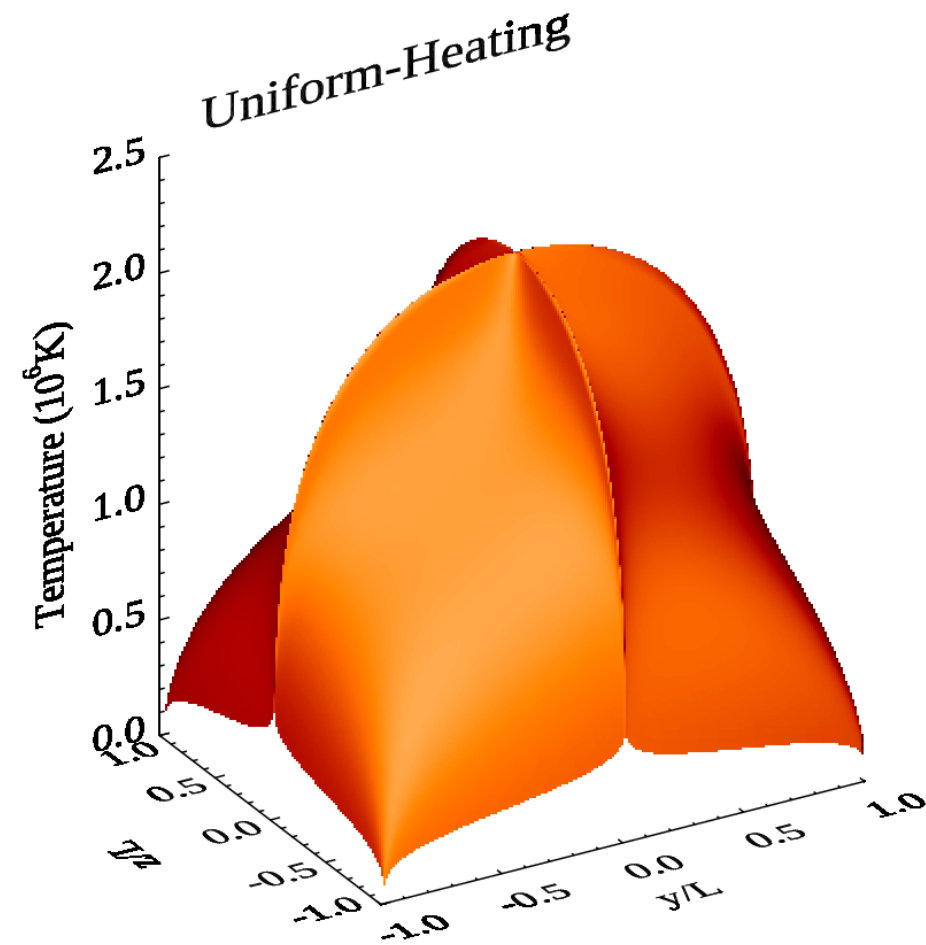
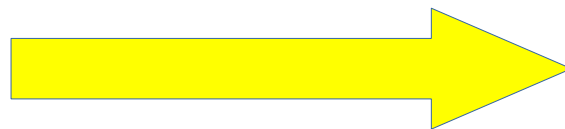
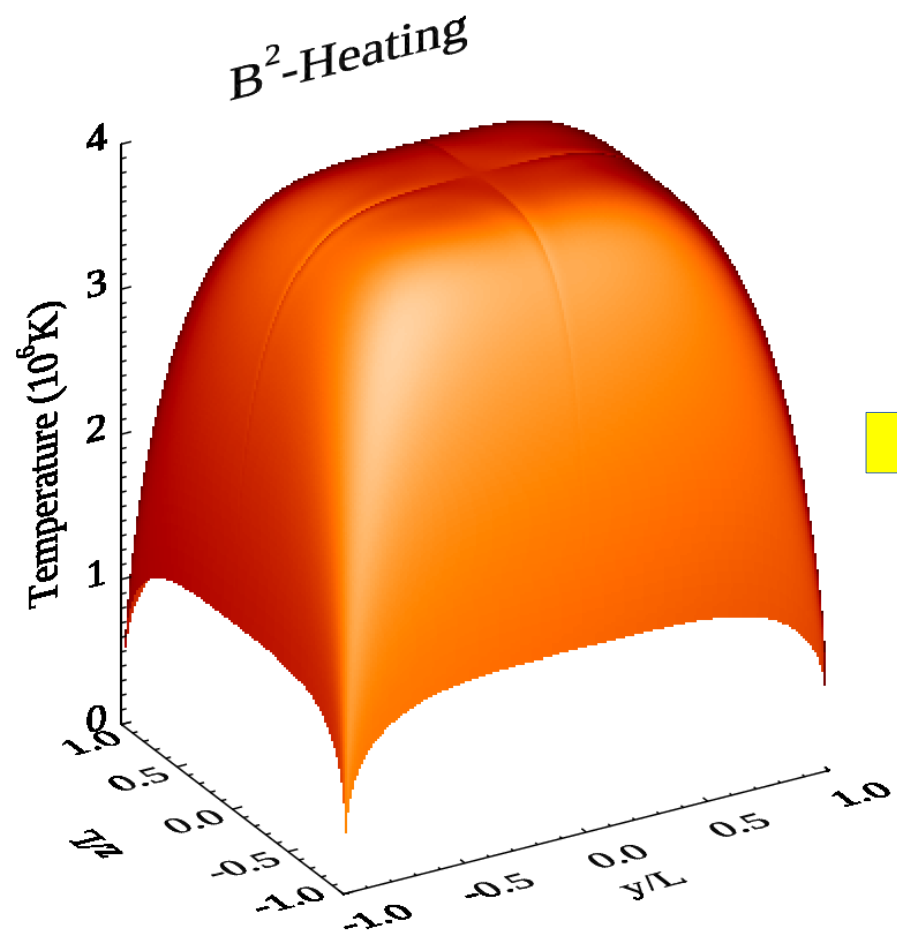
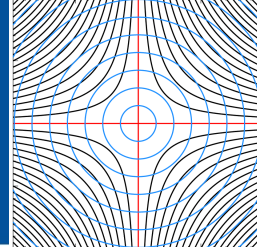


Figure 4. Lare results for the cooling of equilibrium 5 (constant heating: upper panels) and 10 (B^2 heating: lower panels). The left (right) hand plot shows the evolution of the temperature (pressure) at 6 locations along the symmetry line. For constant heating the pressure results lie on top of each other. The dashed and dotted lines are discussed fully in the associated text. In all cases Lare dimensionless units are used.





Paper 3



Natural Heating



Magnetic Field

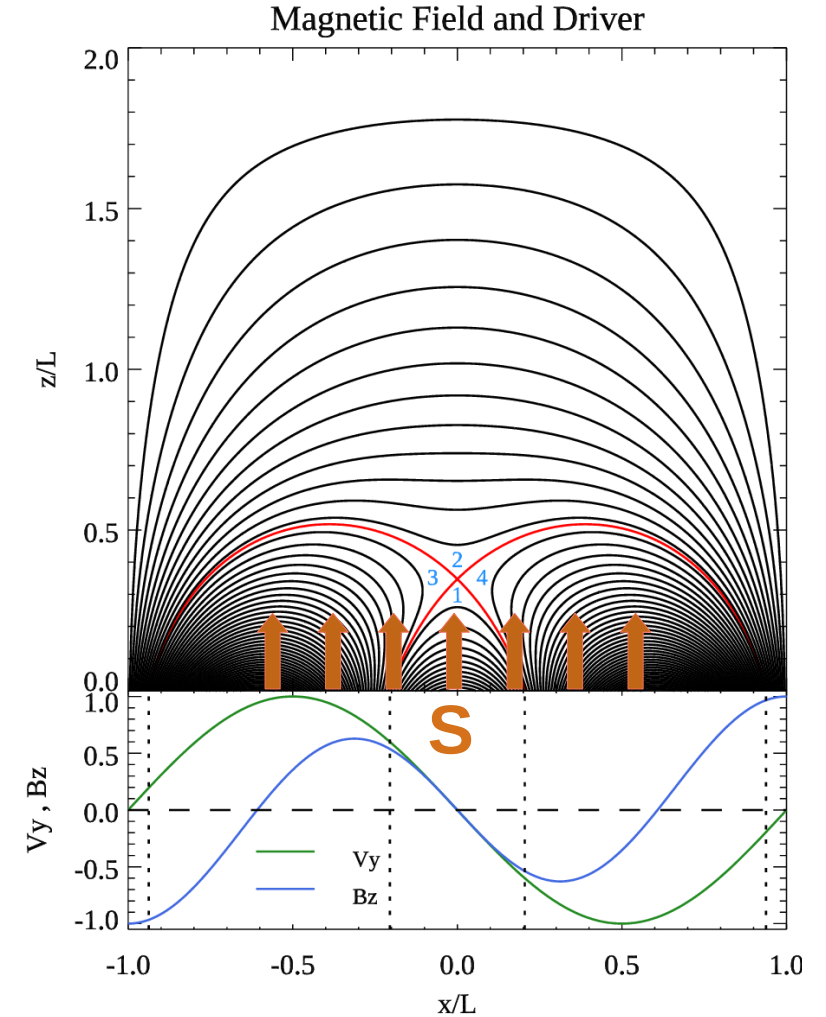
$$\psi = \frac{\cos(kx) \sinh(k[z - L])}{\sinh(kL)} + \alpha \frac{\cos(3kx) \sinh(3k[z - L])}{\sinh(3kL)}$$

$$B_x = -\frac{\partial \psi}{\partial z} \quad B_y = 0 \quad B_z = \frac{\partial \psi}{\partial x}$$

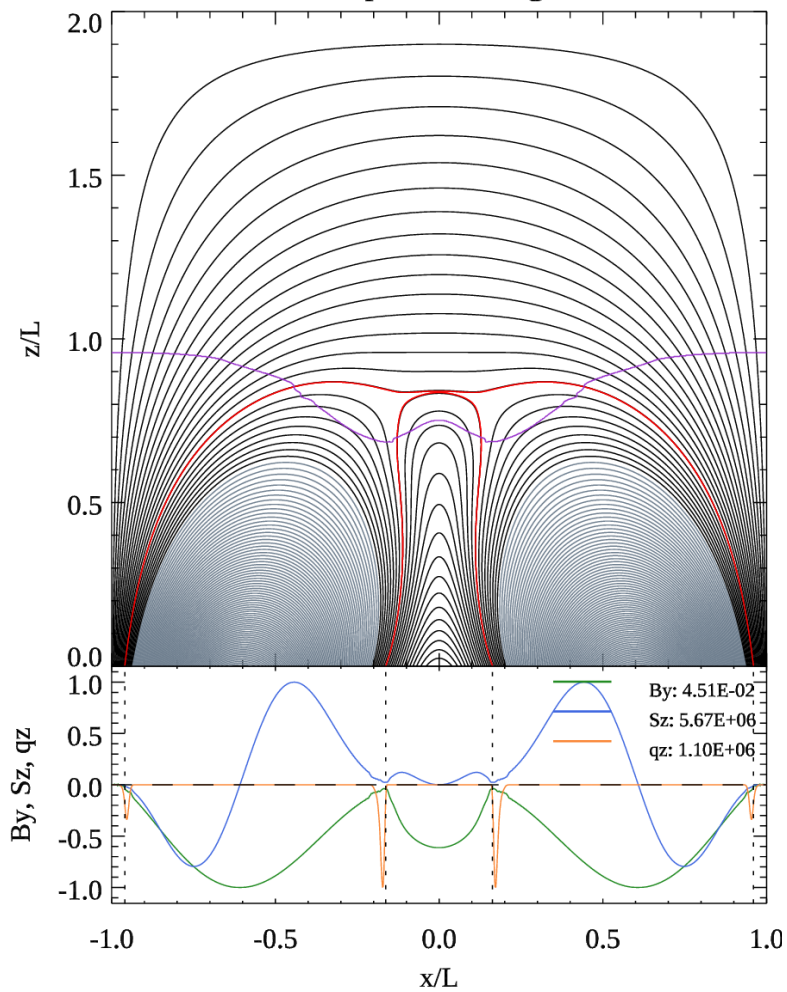
Driver

$$v_y(x, t) = v_{max}(t) \sin\left(\frac{\pi(x+1)}{L}\right)$$

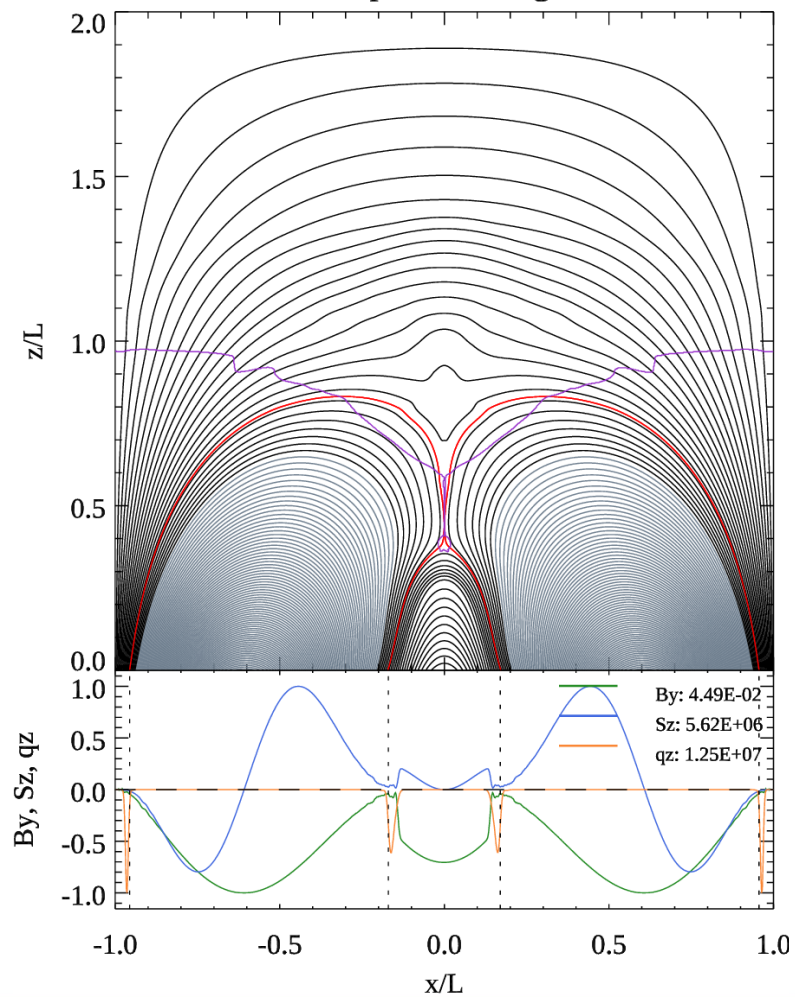
$$\frac{\partial}{\partial t} \left(\frac{\rho v^2}{2} + \frac{B^2}{2\mu_0} + \frac{P}{\gamma - 1} \right) + \nabla \cdot \left(\left[\frac{\rho v^2}{2} + P \frac{\gamma}{\gamma - 1} \right] \mathbf{v} + \mathbf{S} - \mathbf{q} \right) = H - L$$



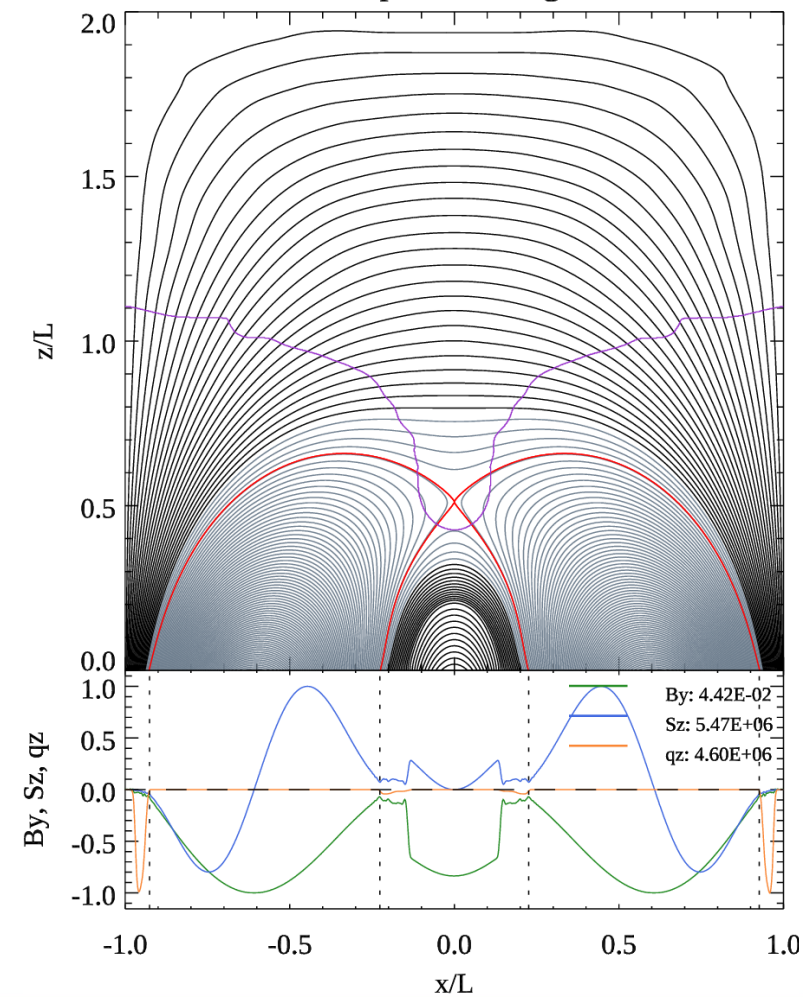
Photospheric Energetics



Photospheric Energetics

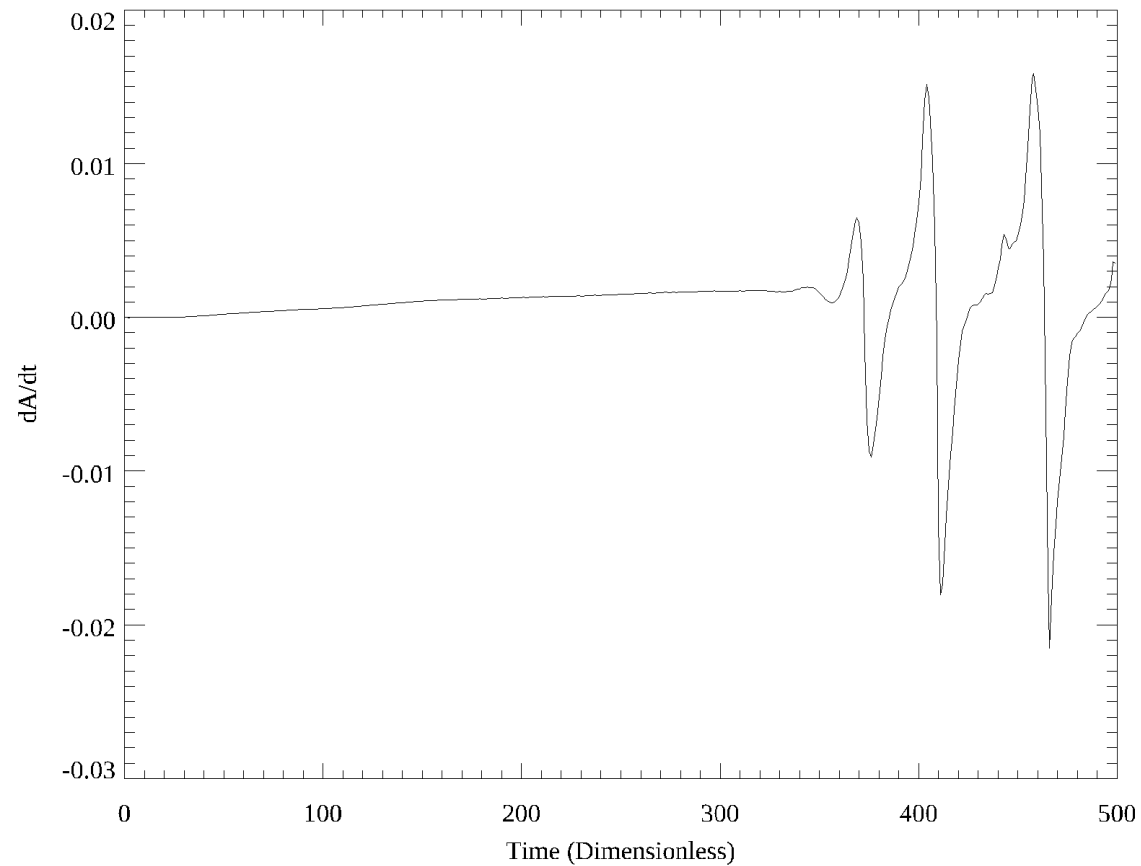


Photospheric Energetics

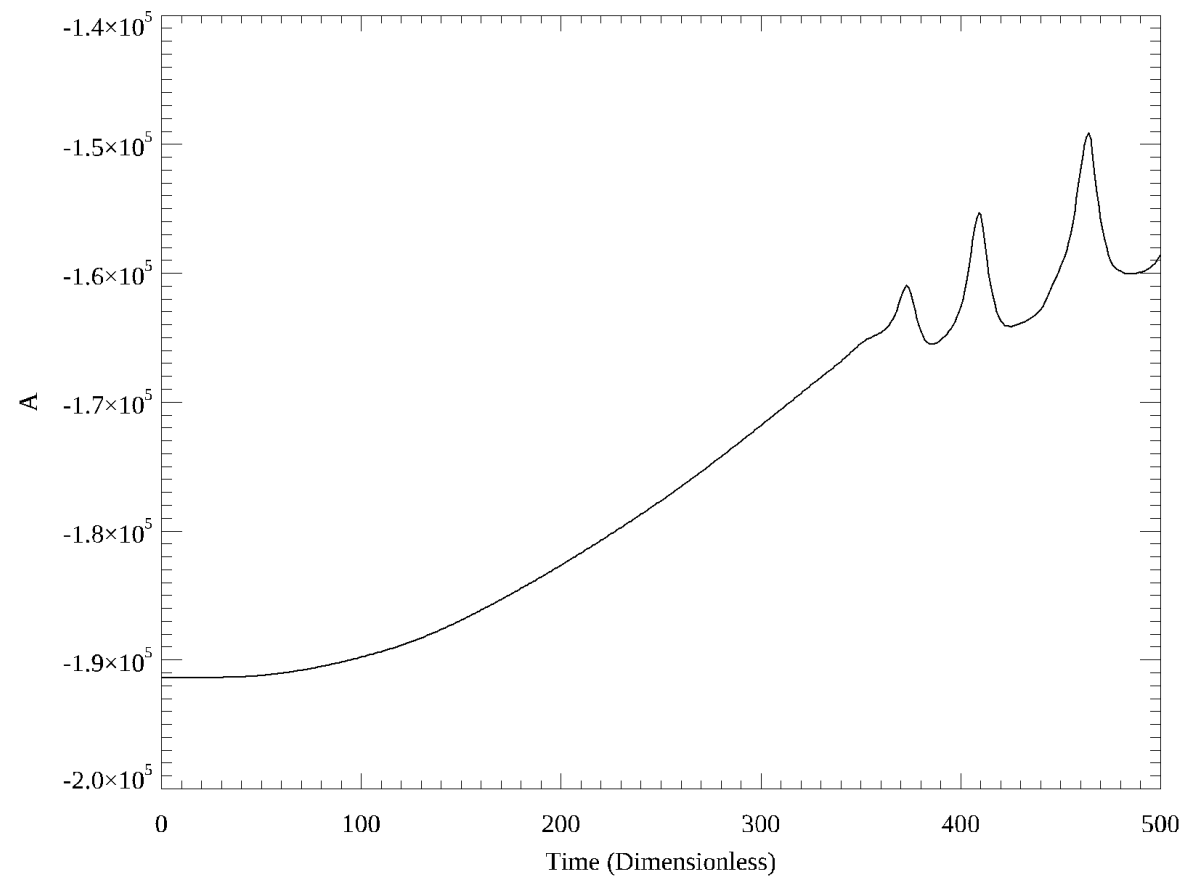


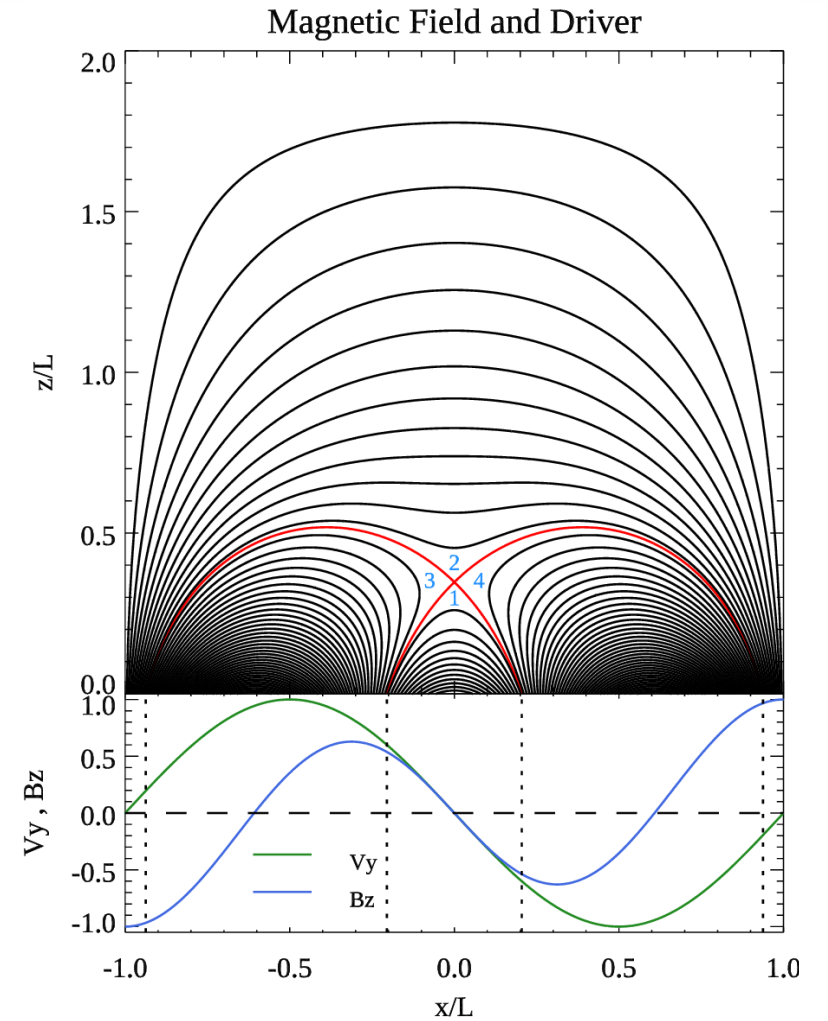
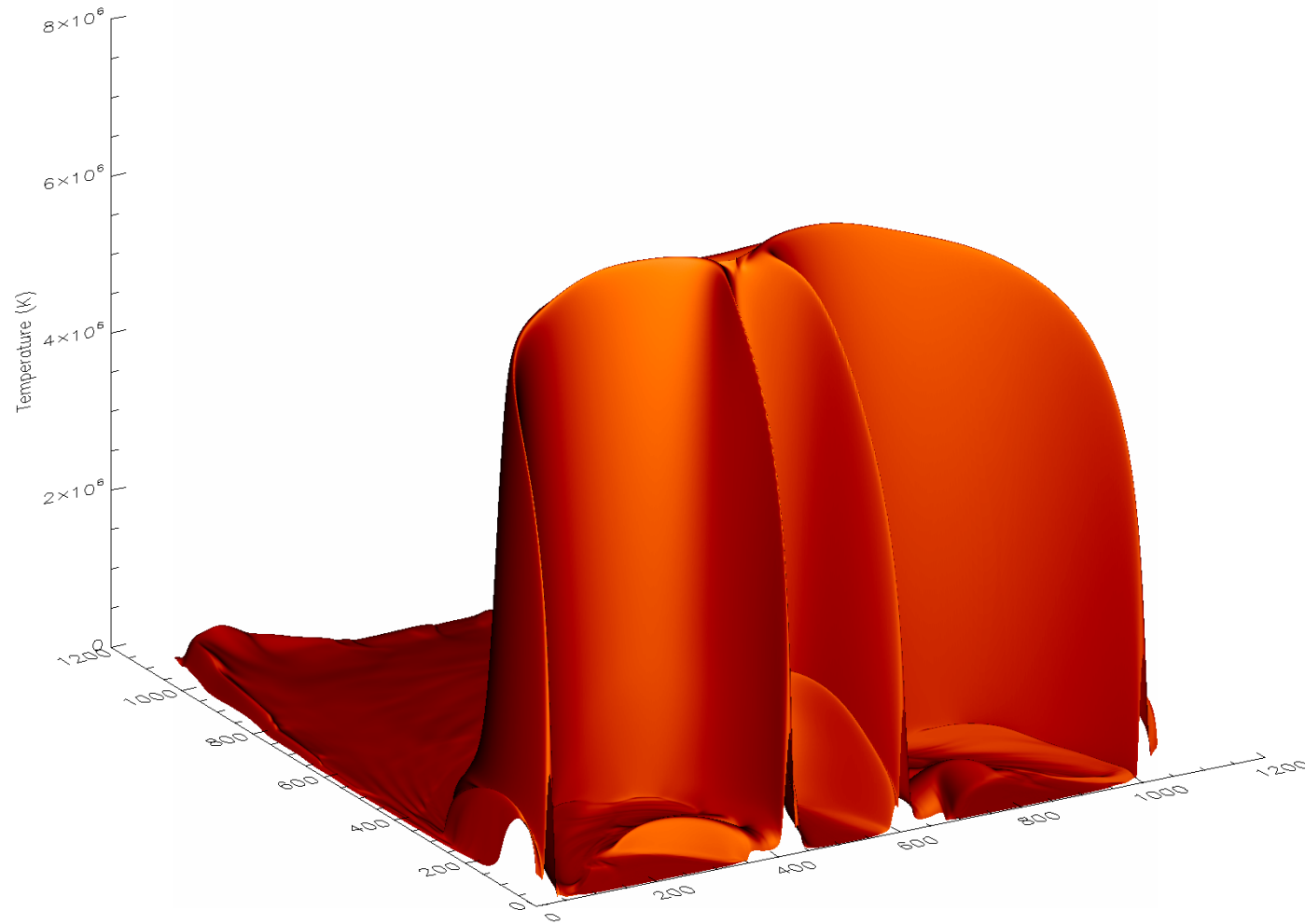


Rate of Change of the Flux Function at the Null Vs Time



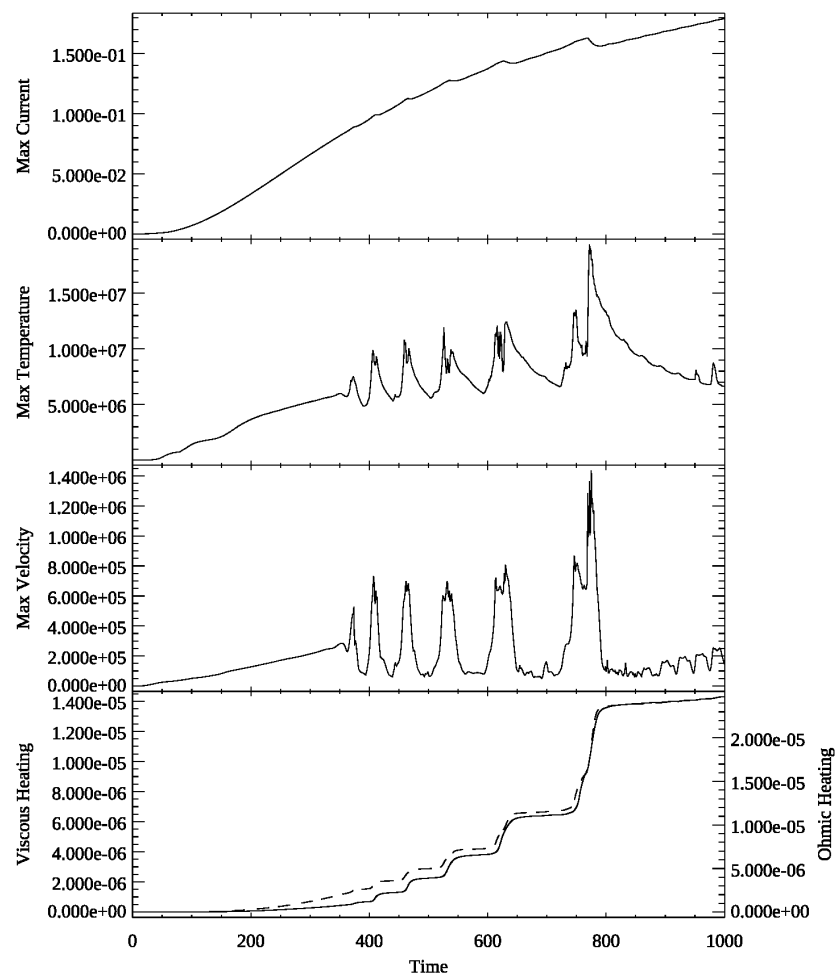
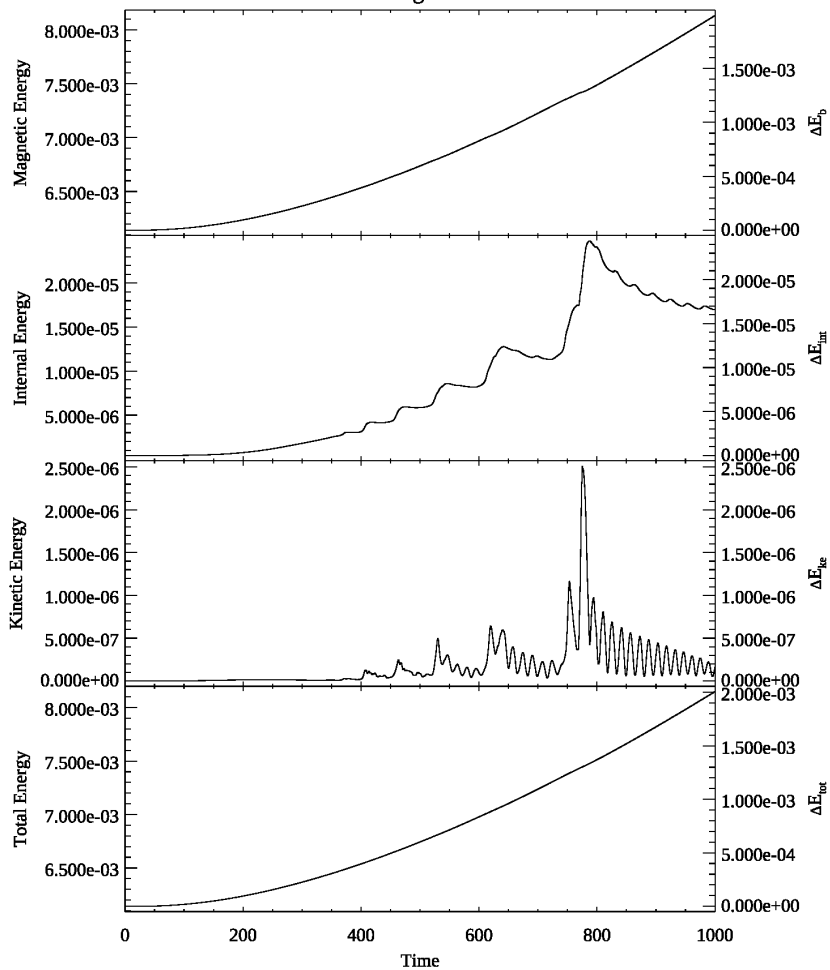
The Flux Function at the Null versus Time



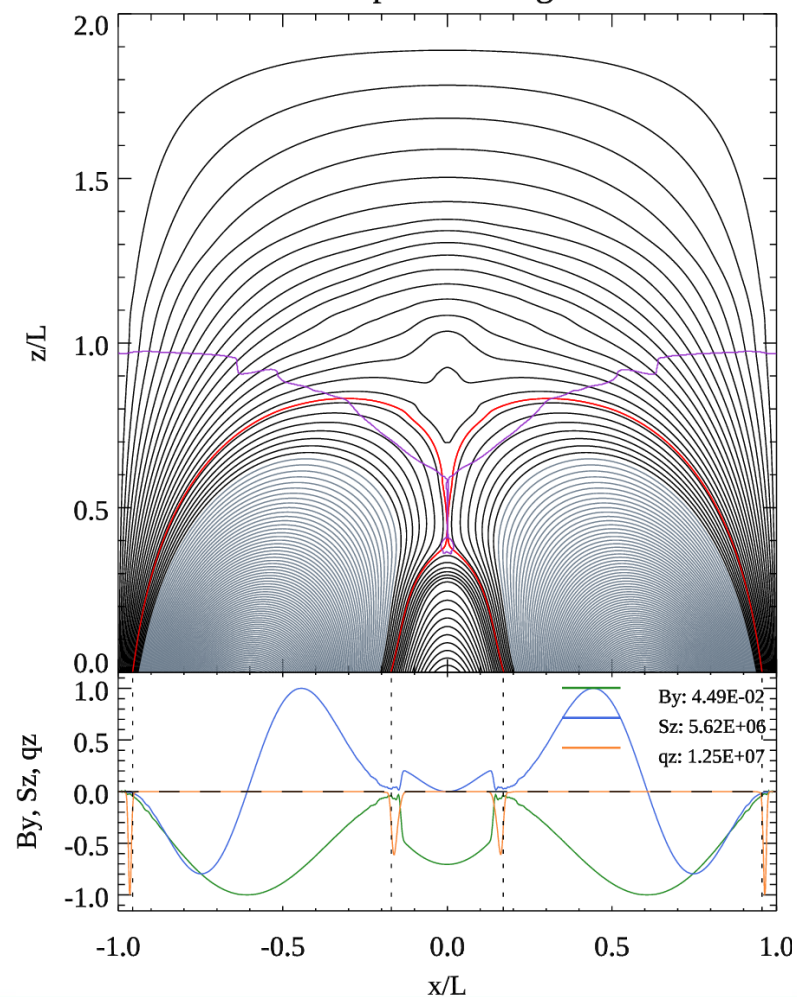




Dominant Energies versus Time

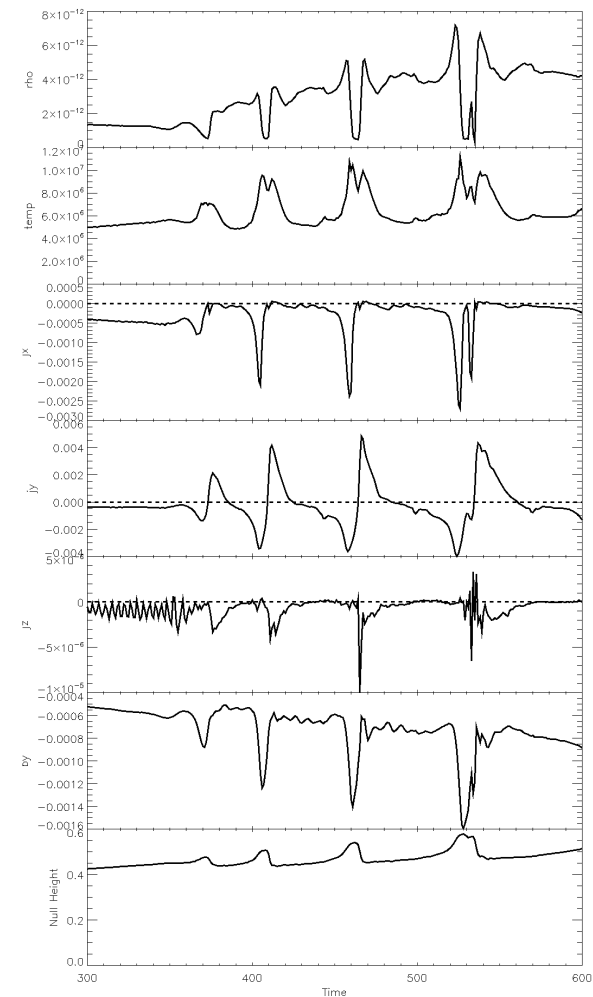
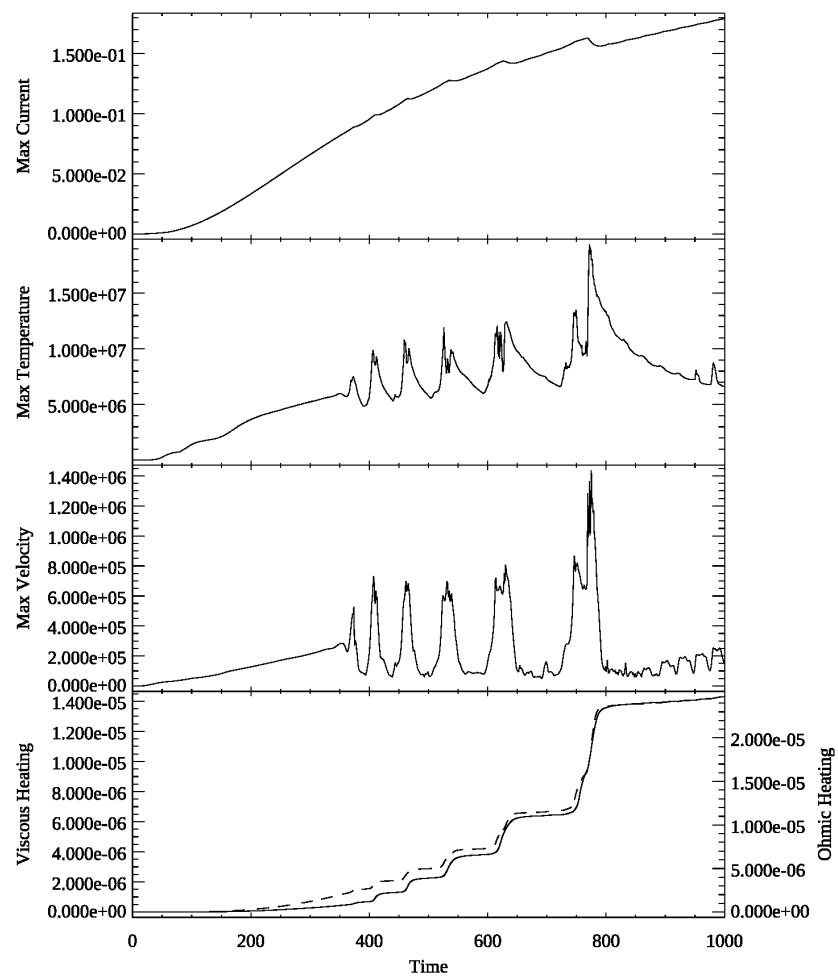
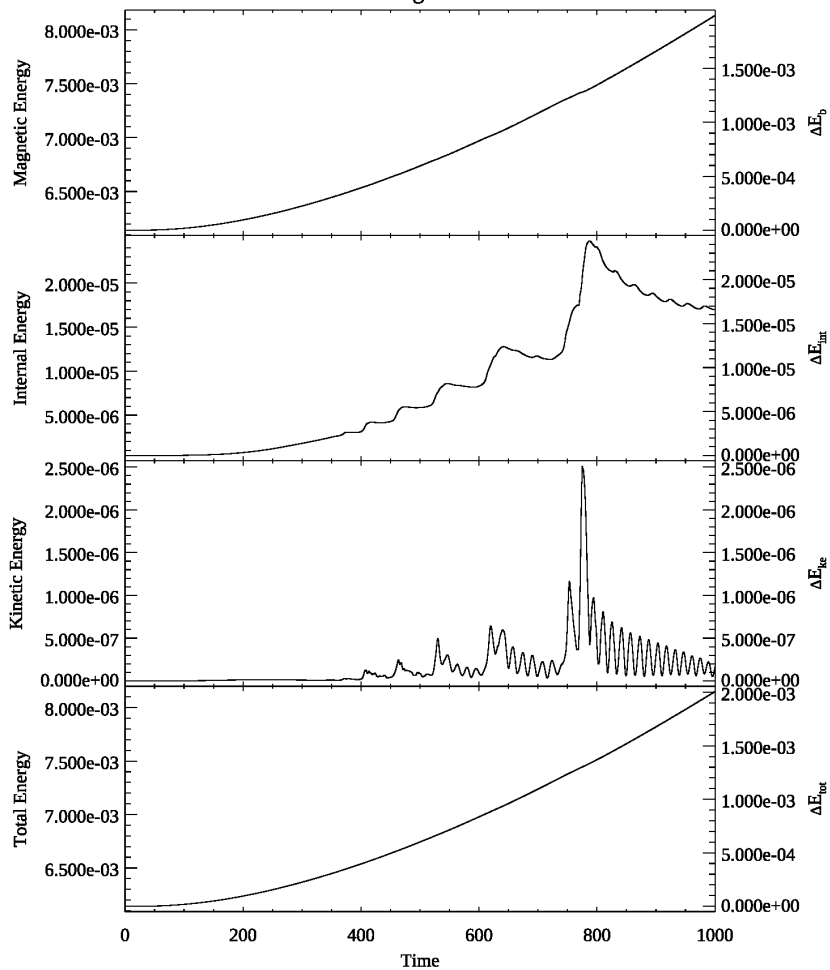


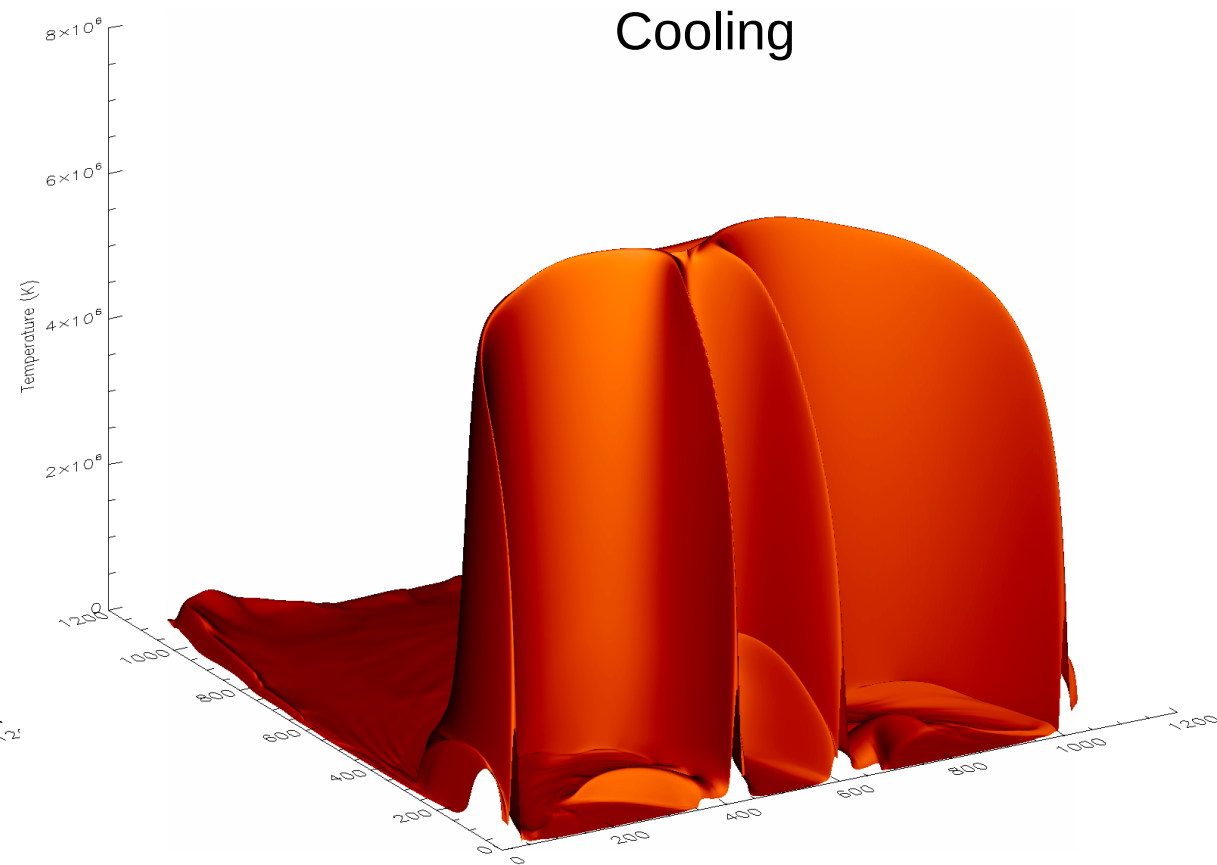
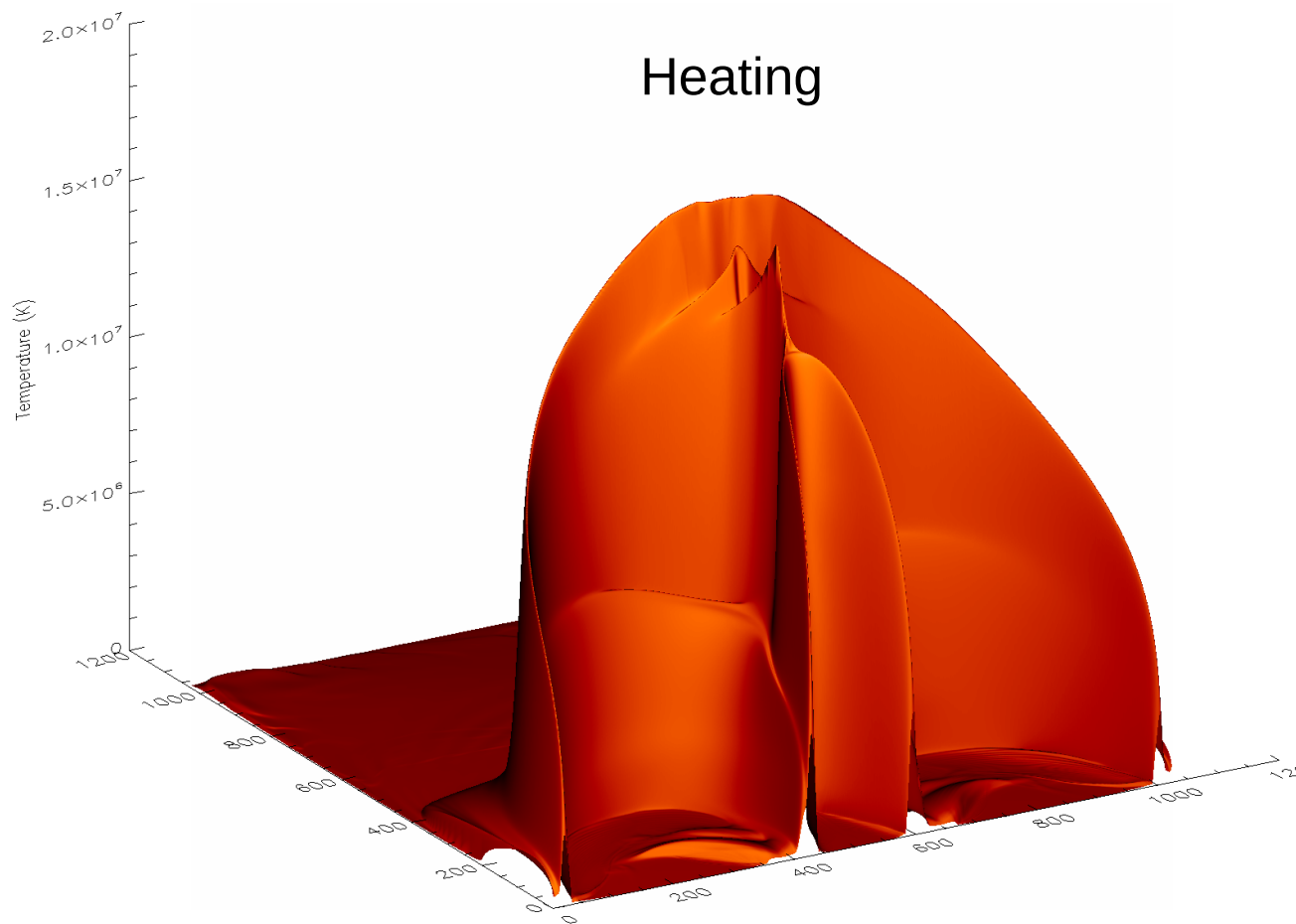
Photospheric Energetics

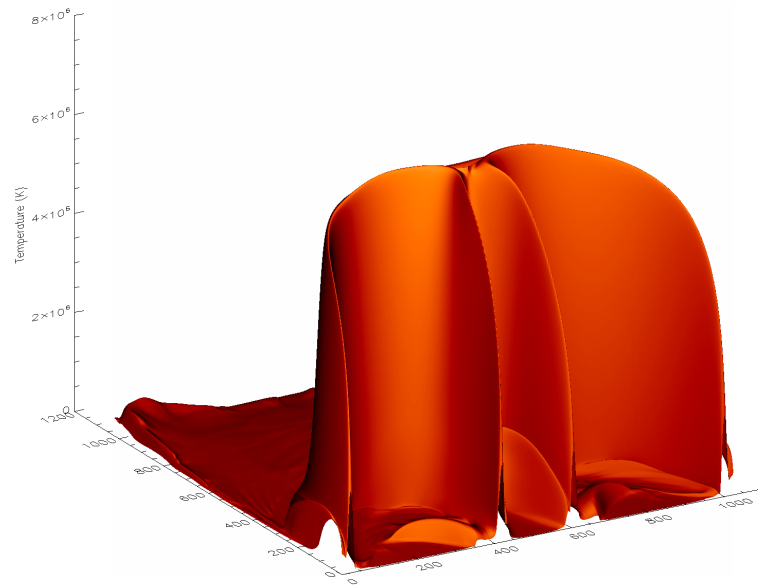




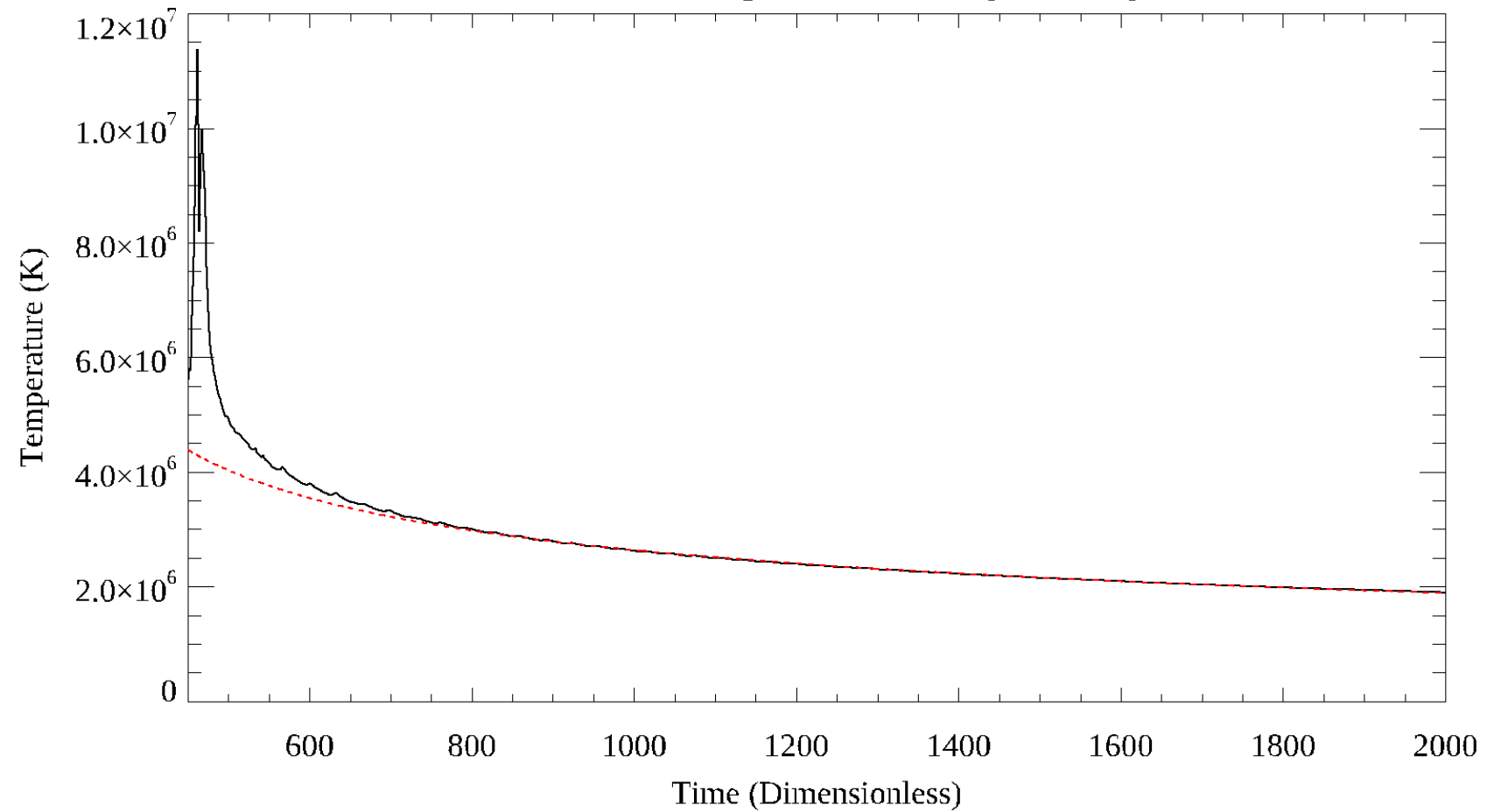
Dominant Energies versus Time







Null Point Temperature During Cooling





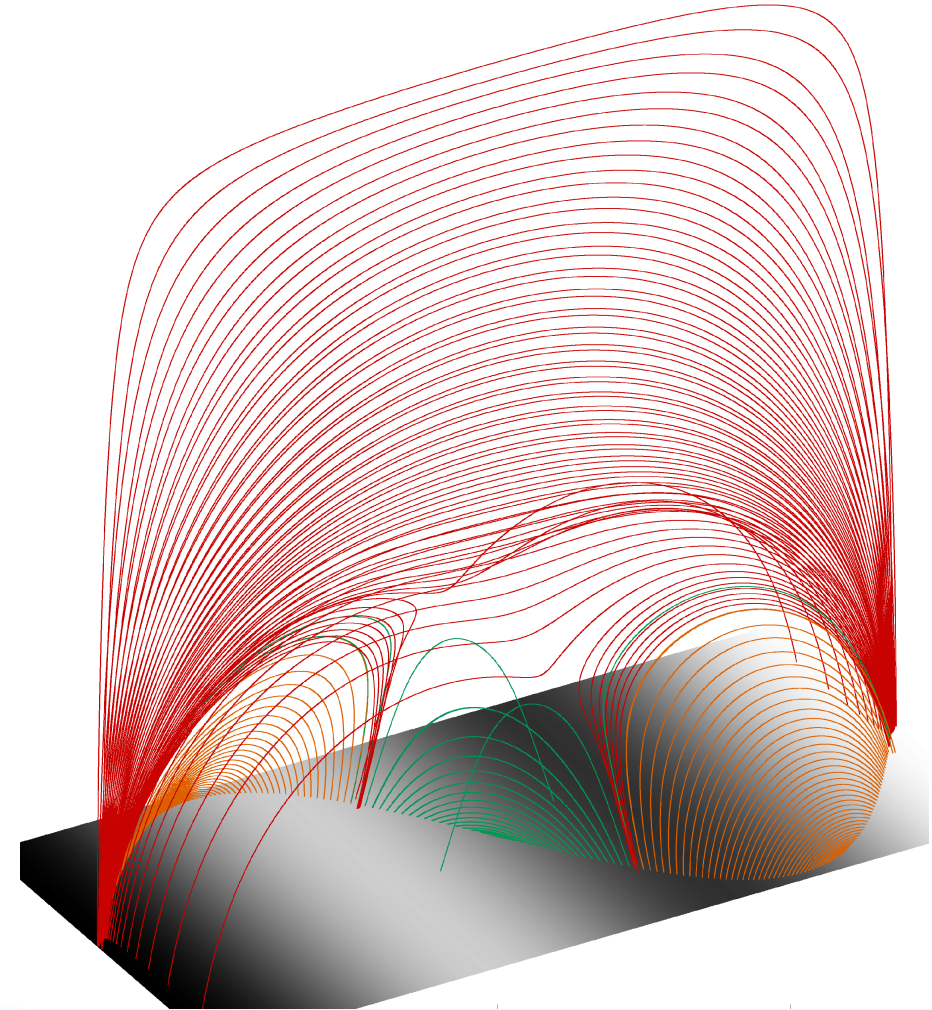
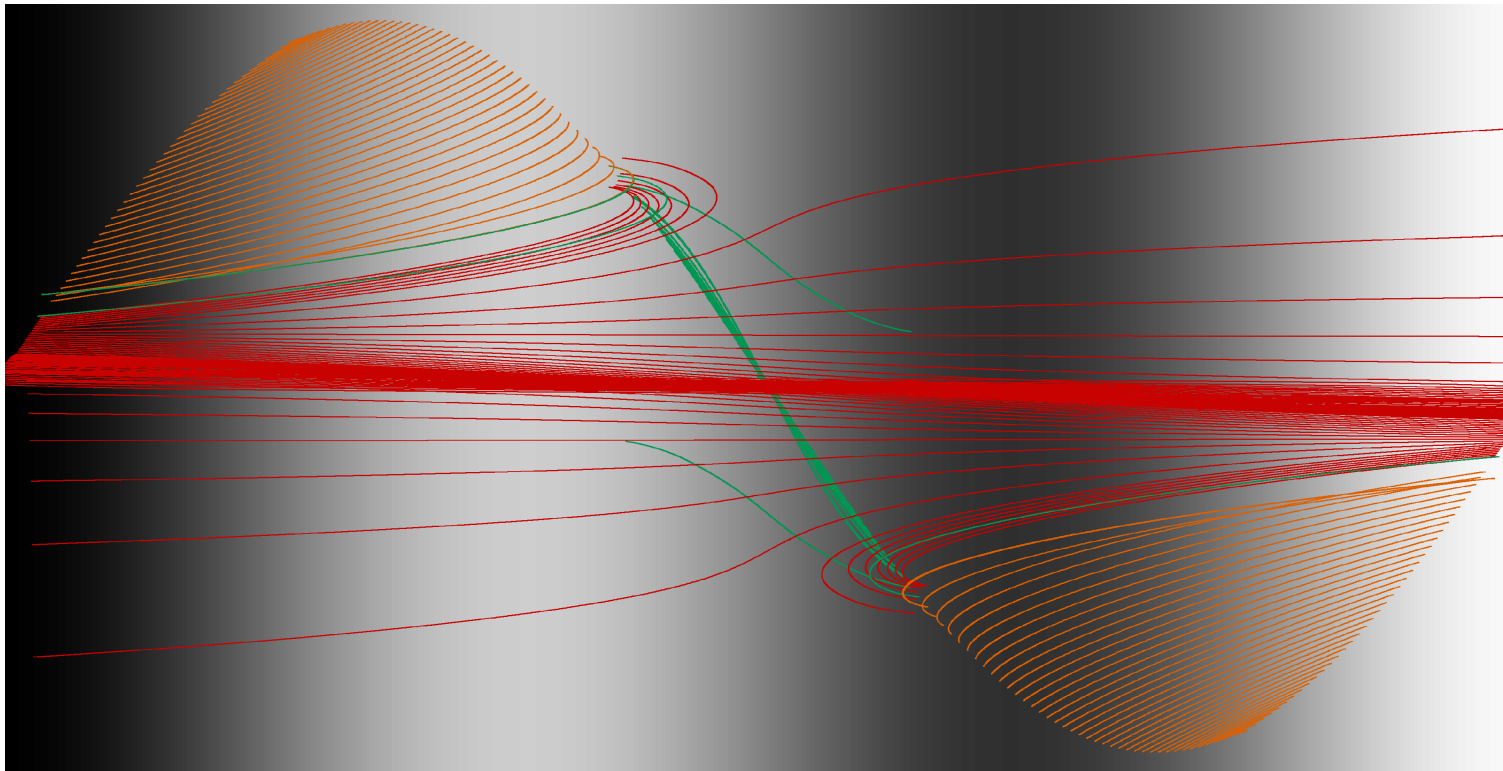
Conclusions

- The geometry of the magnetic field of an X-point significantly influences the equilibrium temperature distribution.
- The equilibrium solution depends heavily on the form of heating; heating at the null leads to singular solutions, with $B_{\min}=0$.
- If we do not heat the null, finite temperatures are produced.
- Null point geometries heavily influence heating **and** cooling.
- **Only infinite simulation resolution will resolve the problem if $B_{\min}=0$. B_{\min} is very small!**
- The null *should* be much hotter if there is a guide field!



Paper 1: Johnson et al. (2024). The thermodynamic response of heating at coronal null points. MNRAS.

Paper 2: Cargill, Hood and Johnson (2025 – very soon). Heating and cooling at a coronal magnetic null. MNRAS.

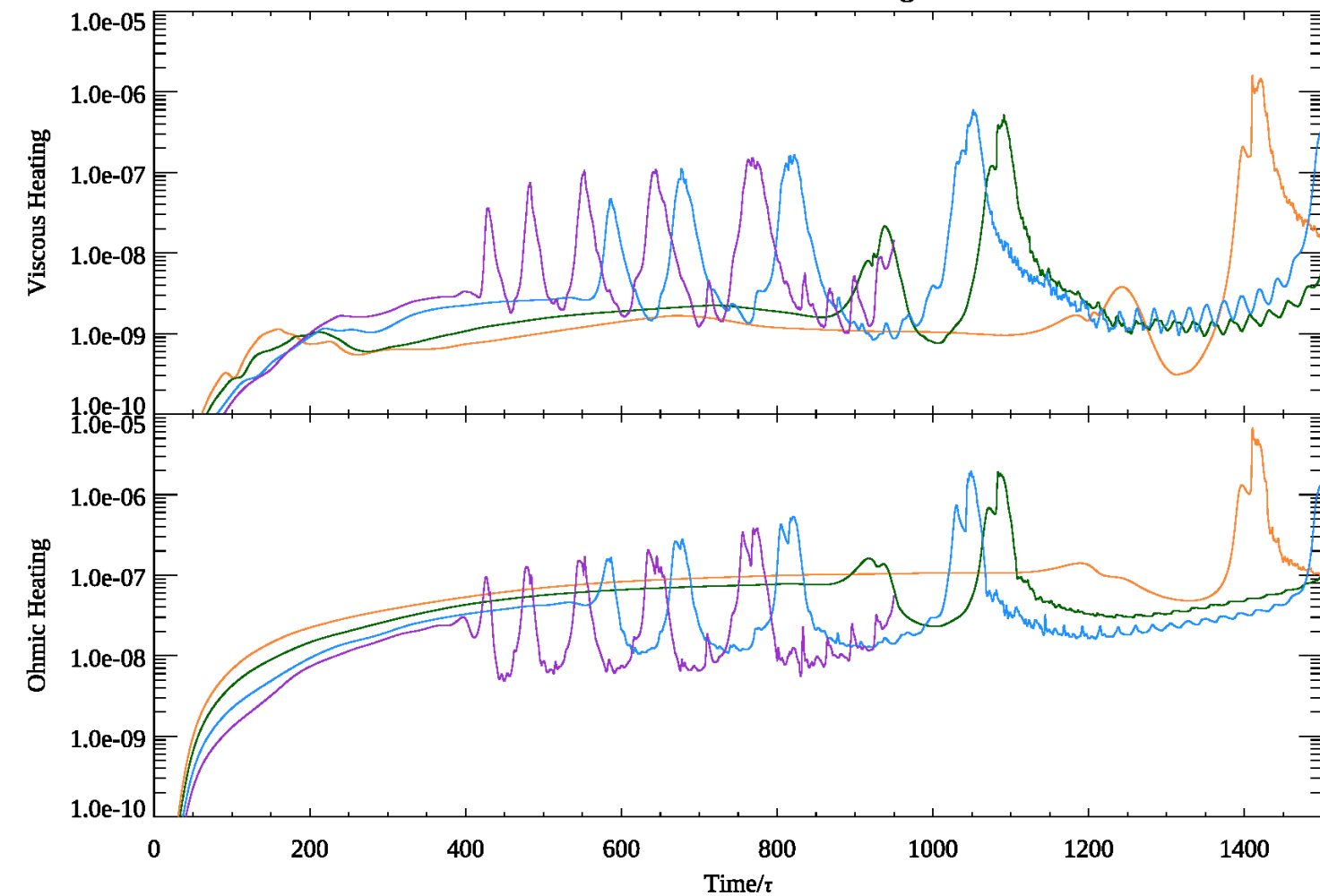




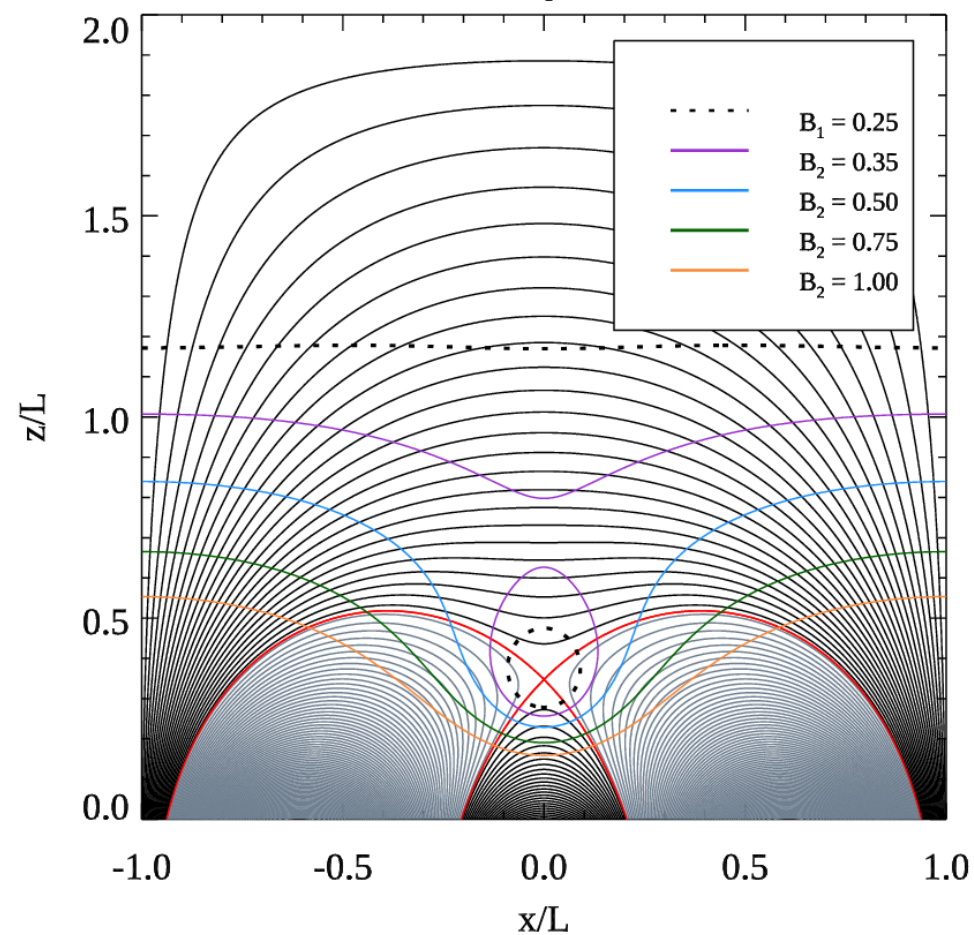
Resistivity and Numerical Nonsense



Ohmic and Viscous Heating



Resistivity Models





Oscillatory Reconnection

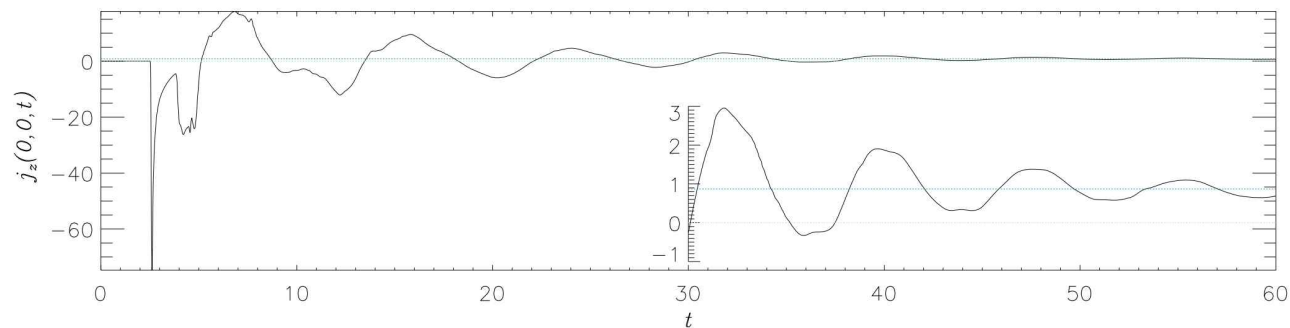
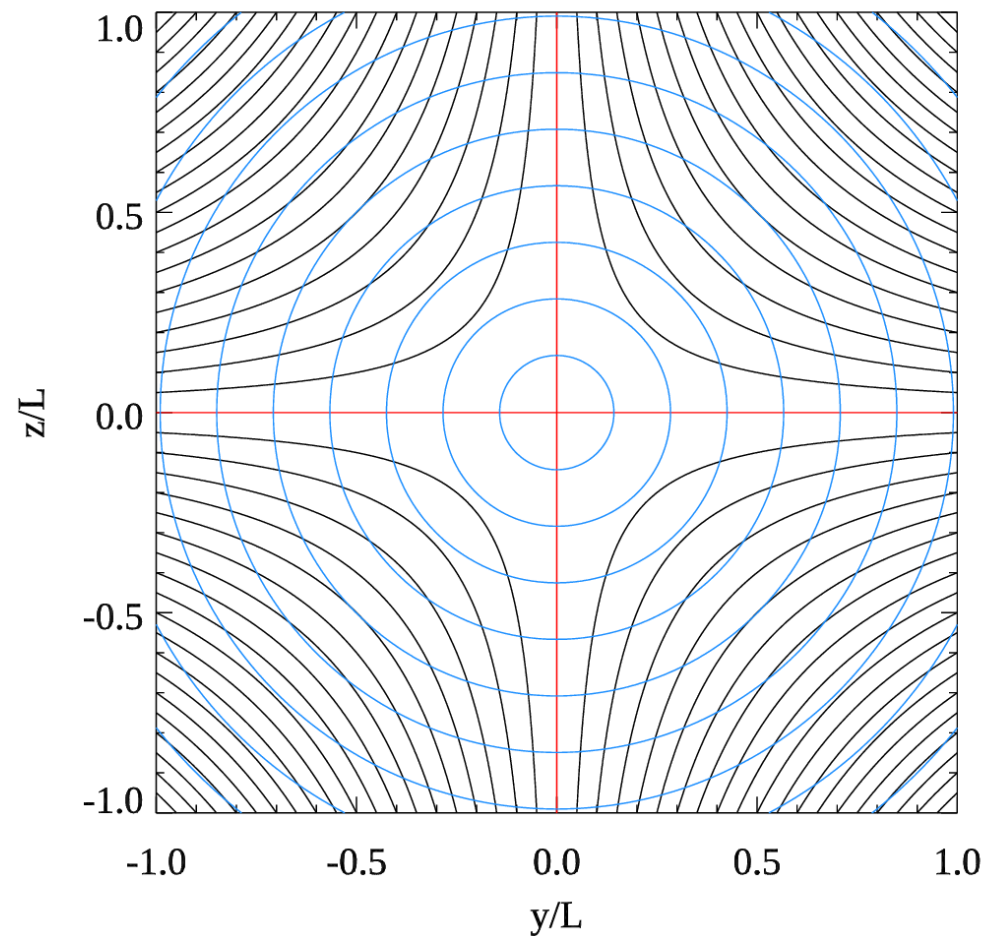


Figure 2. Plot of $j_z(0, 0, t)$ at the null point against time for the baseline simulation ($\eta = 10^{-4}$). The green dashed line denotes $j_z = 0$, with the blue dashed line denoting $j_z = 0.87$, which is the value that the j_z profile tends to.

Image Credit: Talbot et al. (2024)



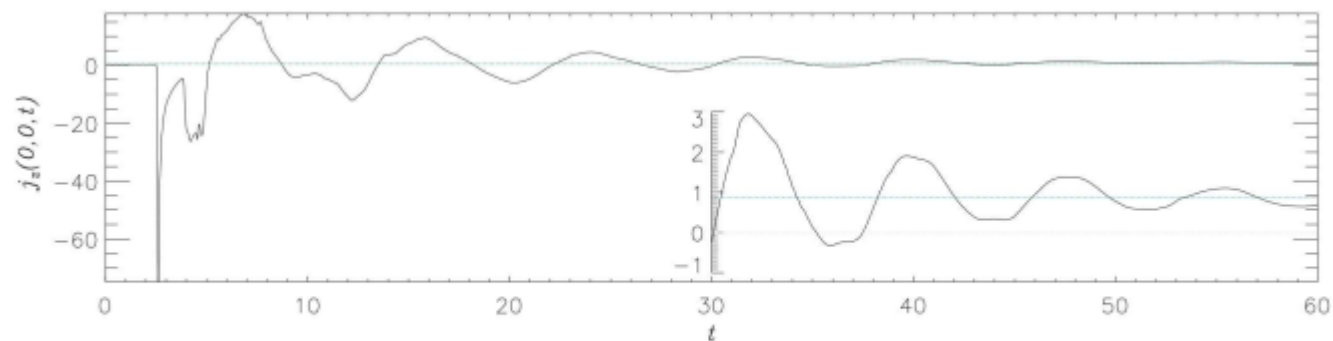
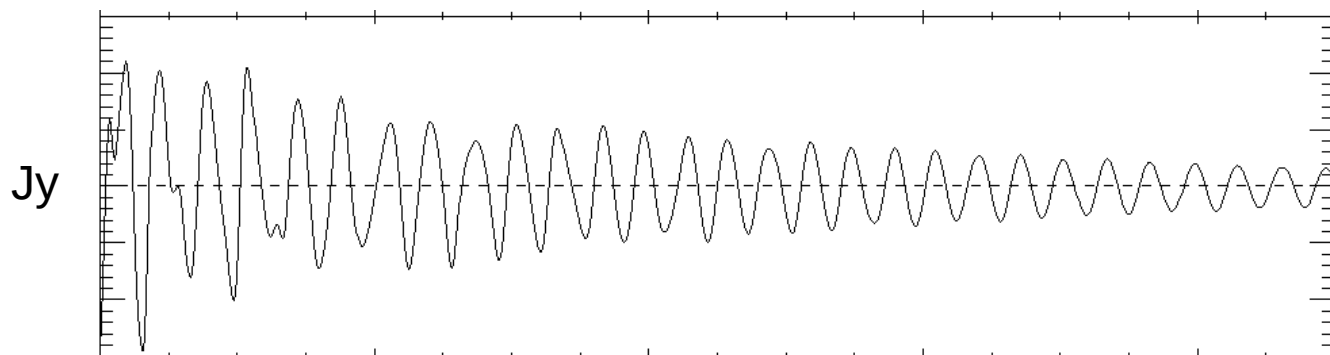
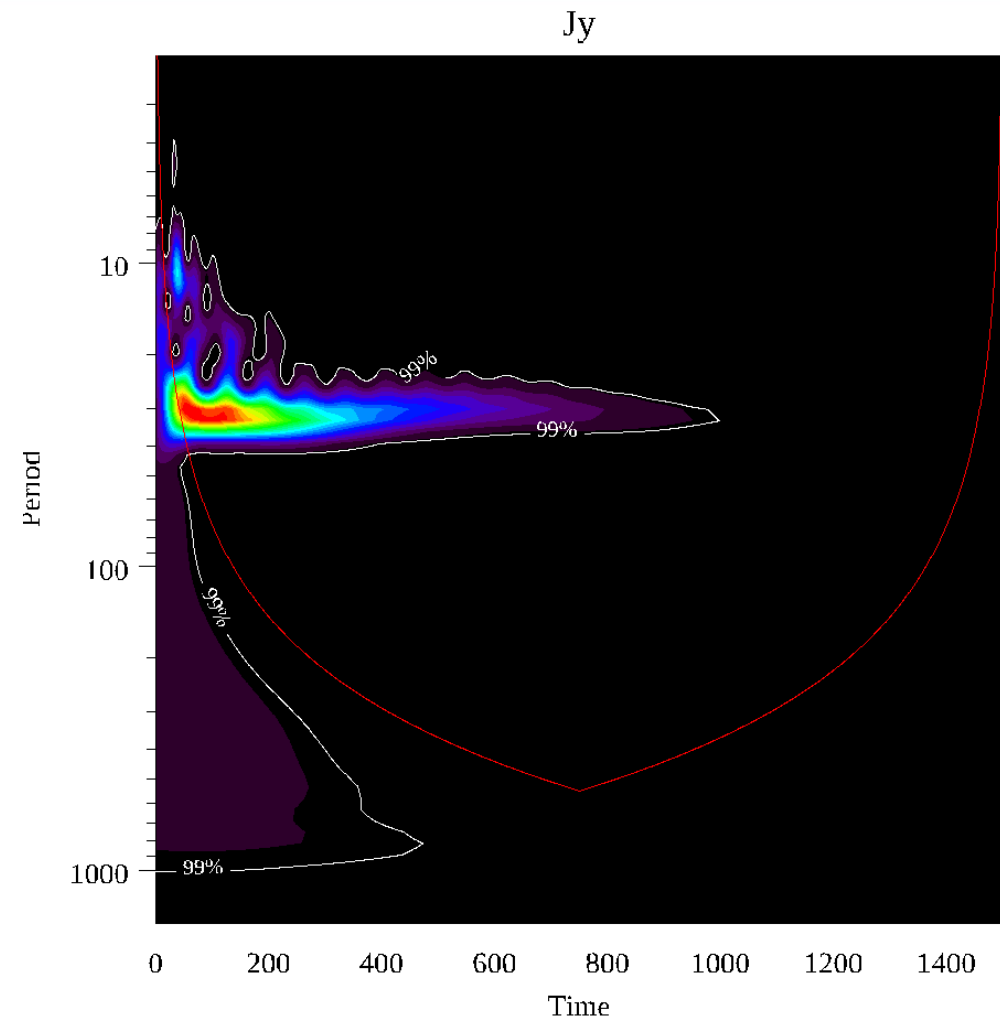


Figure 2. Plot of $j_z(0, 0, t)$ at the null point against time for the baseline simulation ($\eta = 10^{-4}$). The green dashed line denotes $j_z = 0$, with the blue dashed line denoting $j_z = 0.87$, which is the value that the j_z profile tends to.

Image Credit: Talbot et al. (2024)

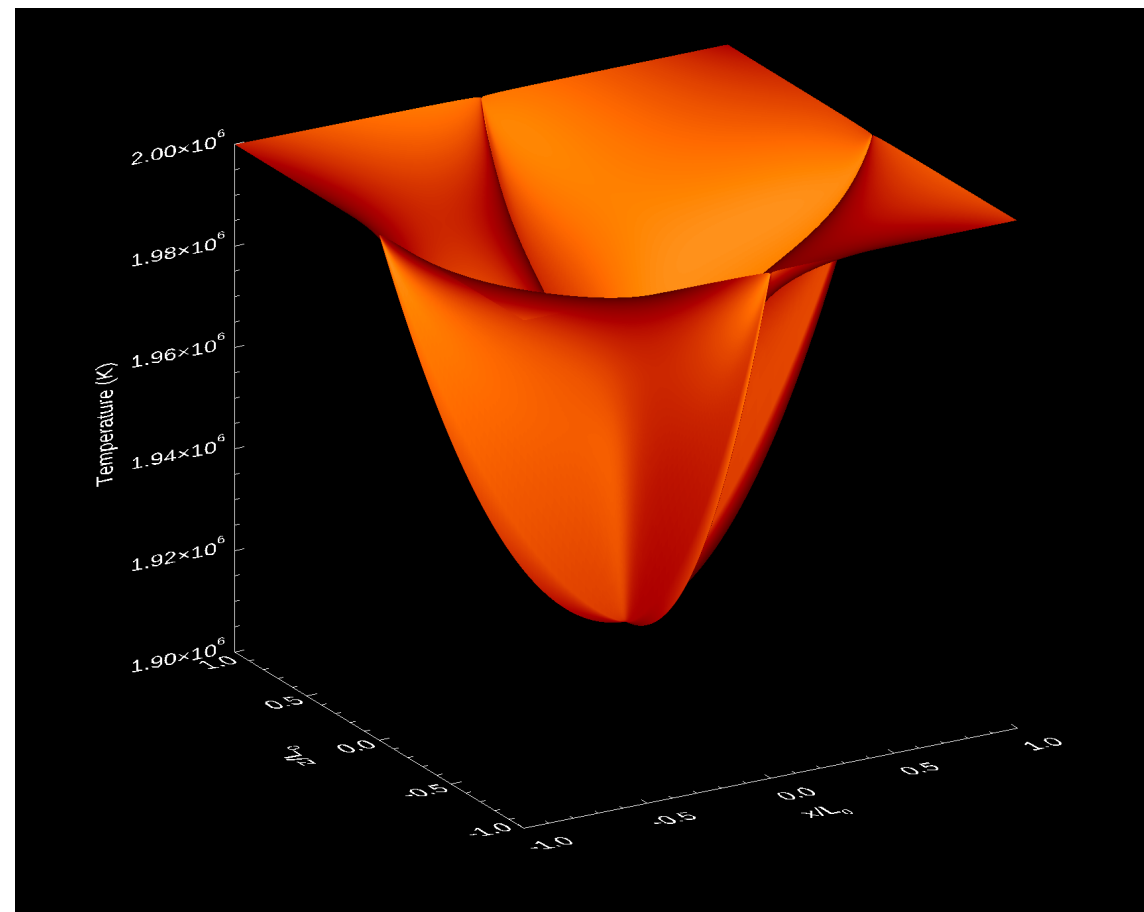
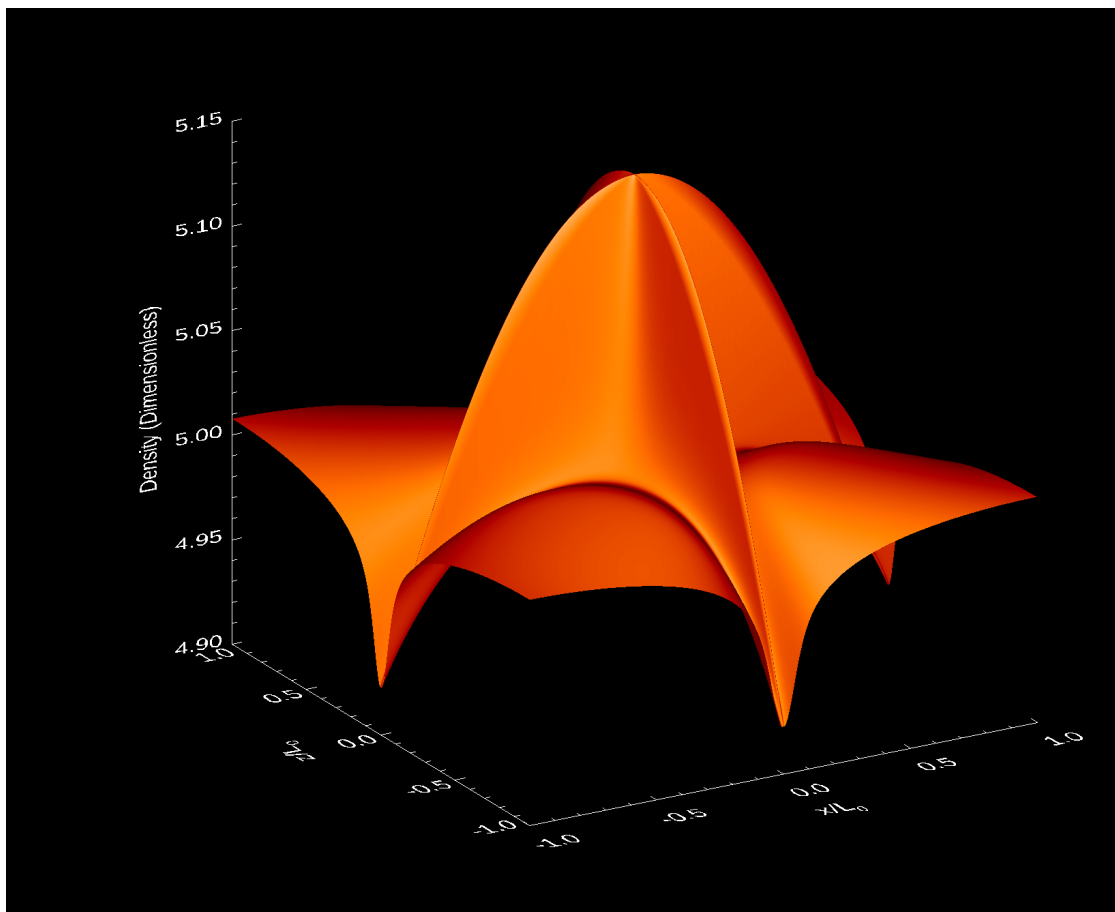


Oscillatory Reconnection (OR) occurs at the null when we stop the driver.





Cold Nulls – Coronal Rain Formation





Question: “Where are all the hot null points in the observations?”

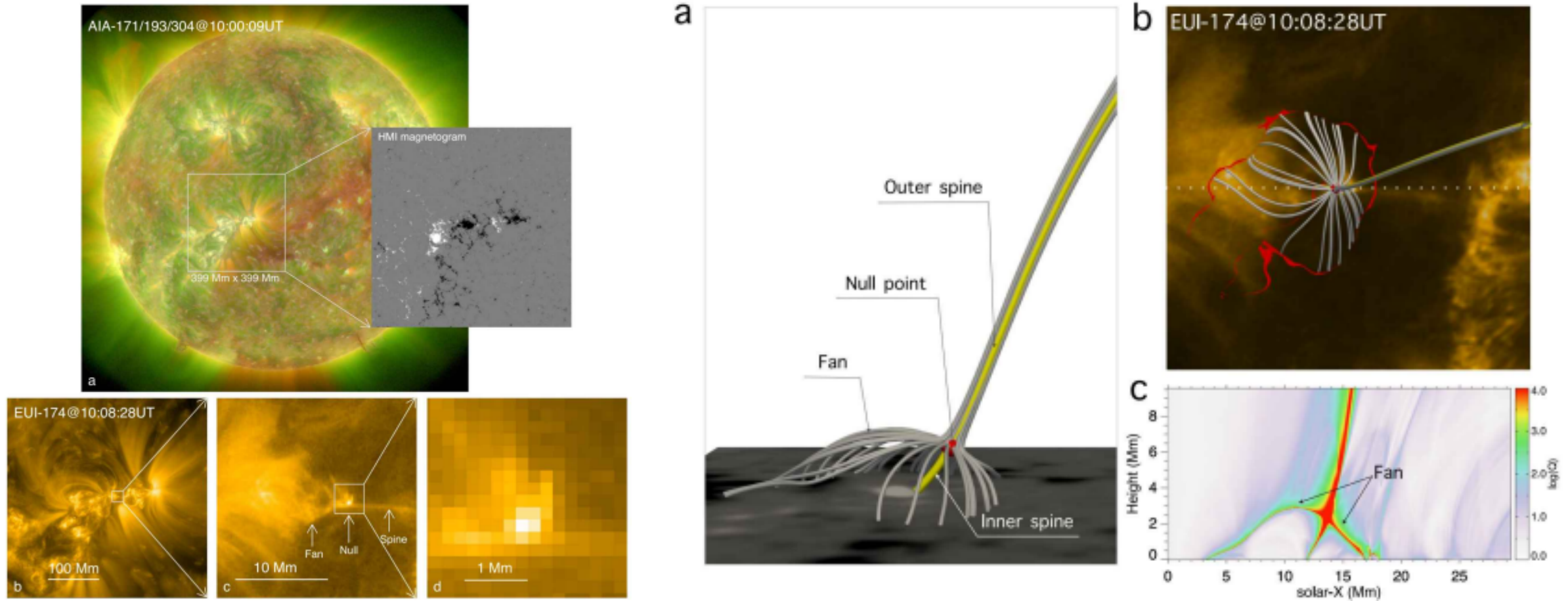


Image credit: Cheng et al. (2023)

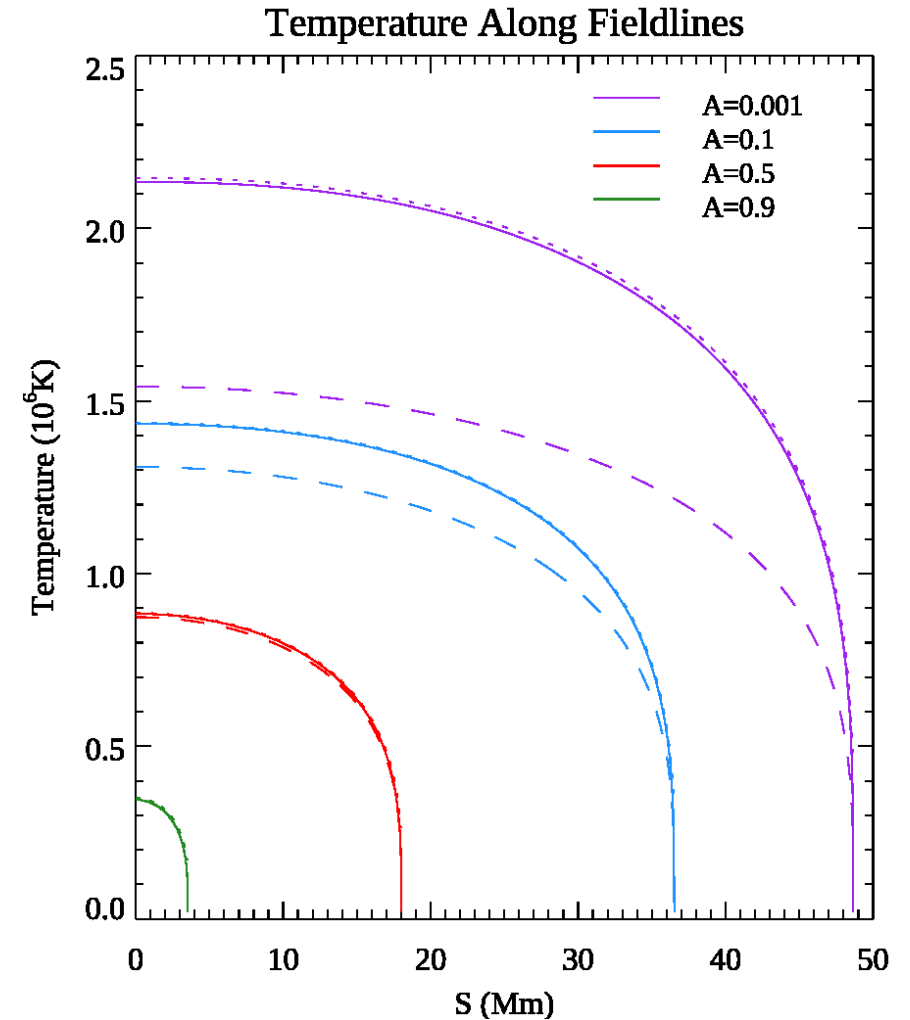


How does the equilibrium temperature compare to straight field?

$$\mathbf{B} \cdot \nabla \left(\frac{\kappa_0 T^{5/2}}{B^2} \mathbf{B} \cdot \nabla T \right) = -H$$

$$\frac{\partial^2 G}{\partial s^2} = -\frac{7HL^2}{2\kappa_0}$$

$$G = G_b - \frac{7HL^2}{4\kappa_0}(S^2 - S_N^2)$$





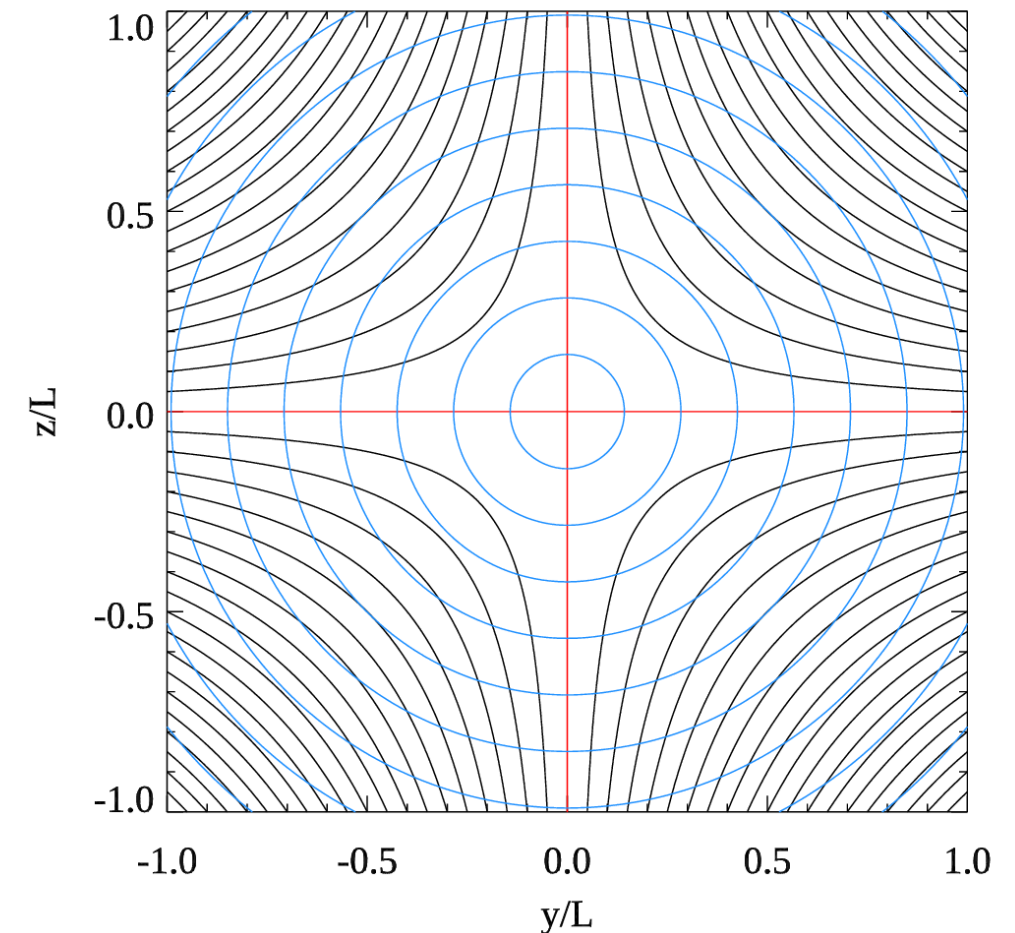
Field Aligned Conduction and the Magnetic Field (why should the null be hotter?)

How does the geometry of a magnetic field influence field aligned thermal conduction? See (Antiochos & Sturrock 1976 and Cargill et al. 2022).

$$-\nabla \cdot \mathbf{q} = \mathbf{B} \cdot \nabla \left(\frac{\kappa_0 T^{5/2}}{B^2} \mathbf{B} \cdot \nabla T \right)$$

$$-\frac{\partial q}{\partial s} = B \frac{\partial}{\partial s} \left(\frac{\kappa_0 T^{5/2}}{B} \frac{\partial T}{\partial s} \right)$$

$$-\frac{\partial q}{\partial s} = \underbrace{\frac{\partial^2}{\partial s^2} \left(\frac{2}{7} \kappa_0 T^{7/2} \right)}_{\text{Straight Field}} + \underbrace{\frac{1}{\mathcal{A}(s)} \frac{\partial \mathcal{A}(s)}{\partial s} \frac{\partial}{\partial s} \left(\frac{2}{7} \kappa_0 T^{7/2} \right)}_{\text{Curved Field – Effective Heating}}$$





Along a Separatrix

$$\mathcal{A}(s) \propto \frac{1}{s}$$

$$-\frac{\partial q}{\partial s} = \frac{\partial^2}{\partial s^2} \left(\frac{2}{7} \kappa_0 T^{7/2} \right) + \frac{1}{\mathcal{A}(s)} \frac{\partial \mathcal{A}(s)}{\partial s} \frac{\partial}{\partial s} \left(\frac{2}{7} \kappa_0 T^{7/2} \right)$$

Straight Field Curved Field – Effective Heating

**You can not cool a null with field
aligned thermal conduction!**

